

## Unexpected Role of the Copper Transporter ATP7A in PDGF-Induced Vascular Smooth Muscle Cell Migration

Takashi Ashino, Varadarajan Sudhahar, Norifumi Urao, Jin Oshikawa, Gin-Fu Chen, Huan Wang, Yuqing Huo, Lydia Finney, Stefan Vogt, Ronald D. McKinney, Edward B. Maryon, Jack H. Kaplan, Masuko Ushio-Fukai and Tohru Fukai

*Circ Res.* 2010;107:787-799; originally published online July 29, 2010;  
doi: 10.1161/CIRCRESAHA.110.225334

*Circulation Research* is published by the American Heart Association, 7272 Greenville Avenue, Dallas, TX 75231  
Copyright © 2010 American Heart Association, Inc. All rights reserved.  
Print ISSN: 0009-7330. Online ISSN: 1524-4571

The online version of this article, along with updated information and services, is located on the  
World Wide Web at:

<http://circres.ahajournals.org/content/107/6/787>

Data Supplement (unedited) at:

<http://circres.ahajournals.org/content/suppl/2010/07/22/CIRCRESAHA.110.225334.DC1.html>

**Permissions:** Requests for permissions to reproduce figures, tables, or portions of articles originally published in *Circulation Research* can be obtained via RightsLink, a service of the Copyright Clearance Center, not the Editorial Office. Once the online version of the published article for which permission is being requested is located, click Request Permissions in the middle column of the Web page under Services. Further information about this process is available in the [Permissions and Rights Question and Answer](#) document.

**Reprints:** Information about reprints can be found online at:  
<http://www.lww.com/reprints>

**Subscriptions:** Information about subscribing to *Circulation Research* is online at:  
<http://circres.ahajournals.org/subscriptions/>

# Unexpected Role of the Copper Transporter ATP7A in PDGF-Induced Vascular Smooth Muscle Cell Migration

Takashi Ashino, Varadarajan Sudhakar, Norifumi Urao, Jin Oshikawa, Gin-Fu Chen, Huan Wang, Yuqing Huo, Lydia Finney, Stefan Vogt, Ronald D. McKinney, Edward B. Maryon, Jack H. Kaplan, Masuko Ushio-Fukai, Tohru Fukai

**Rationale:** Copper, an essential nutrient, has been implicated in vascular remodeling and atherosclerosis with unknown mechanism. Bioavailability of intracellular copper is regulated not only by the copper importer CTR1 (copper transporter 1) but also by the copper exporter ATP7A (Menkes ATPase), whose function is achieved through copper-dependent translocation from *trans*-Golgi network (TGN). Platelet-derived growth factor (PDGF) promotes vascular smooth muscle cell (VSMC) migration, a key component of neointimal formation.

**Objective:** To determine the role of copper transporter ATP7A in PDGF-induced VSMC migration.

**Methods and Results:** Depletion of ATP7A inhibited VSMC migration in response to PDGF or wound scratch in a CTR1/copper-dependent manner. PDGF stimulation promoted ATP7A translocation from the TGN to lipid rafts, which localized at the leading edge, where it colocalized with PDGF receptor and Rac1, in migrating VSMCs. Mechanistically, ATP7A small interfering RNA or CTR1 small interfering RNA prevented PDGF-induced Rac1 translocation to the leading edge, thereby inhibiting lamellipodia formation. In addition, ATP7A depletion prevented a PDGF-induced decrease in copper level and secretory copper enzyme precursor prolysin oxidase (Pro-LOX) in lipid raft fraction, as well as PDGF-induced increase in LOX activity. In vivo, ATP7A expression was markedly increased and copper accumulation was observed by synchrotron-based x-ray fluorescence microscopy at neointimal VSMCs in wire injury model.

**Conclusions:** These findings suggest that ATP7A plays an important role in copper-dependent PDGF-stimulated VSMC migration via recruiting Rac1 to lipid rafts at the leading edge, as well as regulating LOX activity. This may contribute to neointimal formation after vascular injury. Our findings provide insight into ATP7A as a novel therapeutic target for vascular remodeling and atherosclerosis. (*Circ Res.* 2010;107:787-799.)

**Key Words:** vascular remodeling ■ vascular smooth muscle ■ migration ■ copper transporter ■ platelet-derived growth factor

Copper, an essential micronutrient, plays an important role in physiological repair processes including wound healing and angiogenesis, as well as various pathophysiologies including tumor growth, neurodegenerative disease, and atherosclerosis.<sup>1-7</sup> Copper levels are significantly increased in cancer and atherosclerotic lesions.<sup>8,9</sup> Implanting a copper cuff promotes neointima thickening in response to vascular injury,<sup>10</sup> whereas copper chelators prevent this response<sup>11</sup> and tumor growth.<sup>3</sup> Underlying molecular mechanisms remain unclear. Platelet-derived growth factor (PDGF) is a key growth factor to promote neointimal formation and vascular remodeling in vivo primarily through the PDGF receptor- $\beta$  (PDGFR) expressed in vascular smooth muscle cells (VSMCs).<sup>12</sup> VSMC migration

is a critical event for the development of atherosclerosis and restenosis after vascular injury.<sup>12</sup> PDGF-induced cell migration is regulated by actin cytoskeleton, Rac1 activation and translocation to the leading edge.<sup>12,13</sup> However, a role for copper in PDGF-induced VSMC migration has not been demonstrated.

Because excess copper is toxic, copper homeostasis is tightly controlled by regulation of copper uptake, transport and excretion.<sup>1,2</sup> Indeed, under physiological conditions, the level of intracellular free copper is extraordinarily restricted.<sup>14</sup> Copper uptake is mainly mediated by the copper transporter (CTR)1 copper importer, which is involved in embryonic development.<sup>1,15</sup> Once copper enters the cell via

Original received February 23, 2010; resubmission received May 30, 2010; revised resubmission received July 8, 2010; accepted July 16, 2010. In June 2010, the average time from submission to first decision for all original research papers submitted to *Circulation Research* was 14.5 days.

From the Departments of Medicine (Section of Cardiology) and Pharmacology, Center for Cardiovascular Research (T.A., V.S., G.-F.C., R.D.M., T.F., R.D.M.); Department of Pharmacology, Center for Lung and Vascular Biology, Center for Cardiovascular Research (N.U., J.O., R.D.M., M.U.-F.); and Department of Biochemistry and Molecular Genetics (E.B.M., J.H.K.), University of Illinois at Chicago; Cardiovascular Division (H.W., Y.H.), Department of Medicine, University of Minnesota, Minneapolis; and Biosciences Division (L.F.) and X-ray Science Division (L.F., S.V.), Argonne National Laboratory, Ill.

Correspondence to Tohru Fukai, MD, PhD, Departments of Medicine (Section of Cardiology) and Pharmacology, Center for Cardiovascular Research, University of Illinois at Chicago, 835 S Wolcott, M/C868, E403 MSB, Chicago, IL 60612. E-mail tfukai@uic.edu

© 2010 American Heart Association, Inc.

*Circulation Research* is available at <http://circres.ahajournals.org>

DOI: 10.1161/CIRCRESAHA.110.225334

**Non-standard Abbreviations and Acronyms**

<b>ApoE</b>	apolipoprotein E
<b>ATP7A</b>	Menkes ATPase, copper-transporting P-type ATPase
<b>BCS</b>	bathocuproine disulfonate
<b>CTxB</b>	cholera toxin subunit B
<b>CTR1</b>	copper transporter 1, SLC31A1
<b>ICP-MS</b>	inductively coupled plasma mass spectrometry
<b>LOX</b>	lysyl oxidase
<b>LOX-PP</b>	lysyl oxidase pro-peptide
<b>PDGF</b>	platelet-derived growth factor
<b>PDGFR</b>	platelet-derived growth factor receptor- $\beta$
<b>Pro-LOX</b>	proenzyme of lysyl oxidase
<b>HASM</b>	human aortic smooth muscle cell
<b>MASM</b>	mouse aortic smooth muscle cell
<b>RASM</b>	rat aortic smooth muscle cell
<b>siRNA</b>	small interfering RNA
<b>SOD</b>	superoxide dismutase
<b>SXFM</b>	synchrotron-based x-ray fluorescence microscopy
<b>TTM</b>	tetrathiomolybdate
<b>TGN</b>	<i>trans</i> -Golgi network
<b>VSMC</b>	vascular smooth muscle cell

CTR1, it can be delivered into various distinct cellular compartments via ATP7A copper transporting ATPase through the Atox1 copper chaperone.<sup>16,17</sup> ATP7A is ubiquitously expressed and transports copper to the extracellular space or to the selected copper enzymes, which are either secreted from cells, or reside within vesicular compartments.<sup>16,17</sup> When intracellular copper increases, ATP7A translocates from *trans*-Golgi network (TGN) to the plasma membrane or to cytoplasmic vesicles,<sup>16,17</sup> thereby maintaining intracellular copper homeostasis and avoiding copper toxicity. This process requires both copper binding to cytoplasmic regions of ATP7A as well as its catalytic turnover.<sup>18,19</sup>

The biological significance of ATP7A *in vivo* is underscored by Menkes disease, a disorder caused by ATP7A mutations resulting in a marked decrease in copper levels in most tissues except for the kidney and small intestine. Menkes patients show multiple abnormalities secondary to either loss of activity of some secretory copper enzymes or impairment of neuronal activation and other unknown function, leading to death in infancy.<sup>2,20</sup> In vascular tissue, ATP7A is involved in delivering copper to secretory copper enzymes, such as superoxide dismutase (SOD)<sup>3</sup> and proenzyme of lysyl oxidase (Pro-LOX).<sup>17,20–22</sup> After secretion, Pro-LOX is processed and activated by proteolysis to a mature active 32-kDa enzyme (LOX) and an 18-kDa propeptide (LOX-PP), both of which are expressed in vascular tissue.<sup>22,23</sup> LOX is known to be critical for vascular extracellular matrix maturation by regulating the cross-linking of collagens or elastin. Of note, LOX is stimulatory but LOX-PP is inhibitory for cell migration.<sup>23–25</sup> No information is available regarding a role of ATP7A in PDGF-mediated vascular migration and remodeling.

Here, we demonstrate the novel role of ATP7A in PDGF-induced VSMC migration. PDGF stimulation promotes ATP7A translocation from the TGN to lipid rafts which localize at the leading edge in migrating VSMC, thereby promoting lamellipodia formation through recruiting Rac1, in a CTR1-dependent manner. This is associated with a decrease in cellular copper and secretory copper enzyme precursor prollysyl oxidase in caveolae/lipid rafts, which may contribute to activation of LOX. *In vivo*, ATP7A expression is markedly increased and copper accumulation is observed at neointimal VSMC in wire injury model. These findings provide insight into ATP7A as potential therapeutic targets for vascular remodeling and development of atherosclerosis.

## Methods

An expanded Methods section is available in the Online Data Supplement at <http://circres.ahajournals.org>.

### Detergent-Free Purification of Caveolin-Rich Membrane Fractions

Caveolae/lipid raft fractions were separated by the sodium carbonate-based detergent-free method.

### Copper Measurements

Copper contents were analyzed by inductively coupled plasma mass spectrometry (ICP-MS) using a PlasmaQuad3, as reported previously.<sup>26</sup>

### Vascular Injury

Animal protocols were approved by the Animal Care and Use Committee of the University of Illinois at Chicago and University of Minnesota. Wire-induced injury of the carotid artery in apolipoprotein (Apo)E-deficient atherosclerotic mice was performed, as reported previously.<sup>27</sup>

### Synchrotron X-Ray Fluorescence Microscopy

Sections (5- $\mu$ m thick) of formalin-fixed, paraffin-embedded, wire-injured femoral artery were used. For x-ray imaging, the sections (5- $\mu$ m thick) of formalin-fixed, paraffin-embedded, wire-injured femoral artery were prepared on silicon nitride windows (Silson), as reported previously.<sup>28</sup>

## Results

### Expression of the ATP7A Copper Transporter and the CTR1 Copper Importer in VSMCs

RT-PCR analysis of rat, mouse, and human aortic smooth muscle cells (RASMs, HASMs, and MASMs) detected both ATP7A and CTR1 expression (Figure 1A). Western analysis with anti-ATP7A antibody showed expression of ATP7A with a 178-kDa protein in whole cell lysates of RASMs, HASMs, and MASMs (Figure 1B).<sup>16,17</sup> By contrast, CTR1 protein was not detected in whole cell lysates, but in caveolae/lipid rafts fraction, by specific anti-CTR1 antibody, as shown later (Figure 5A; Online Figure V, A and B).

### ATP7A Is Involved in PDGF-Induced VSMC Migration in a Copper-Dependent Manner

We next examined the role of ATP7A in VSMC migration. Modified Boyden chamber assays demonstrated that knock-down of endogenous ATP7A expression with small interfering (si)RNA significantly inhibited PDGF-stimulated migration in VSMCs (Figure 1C and Online Figure I). Because the

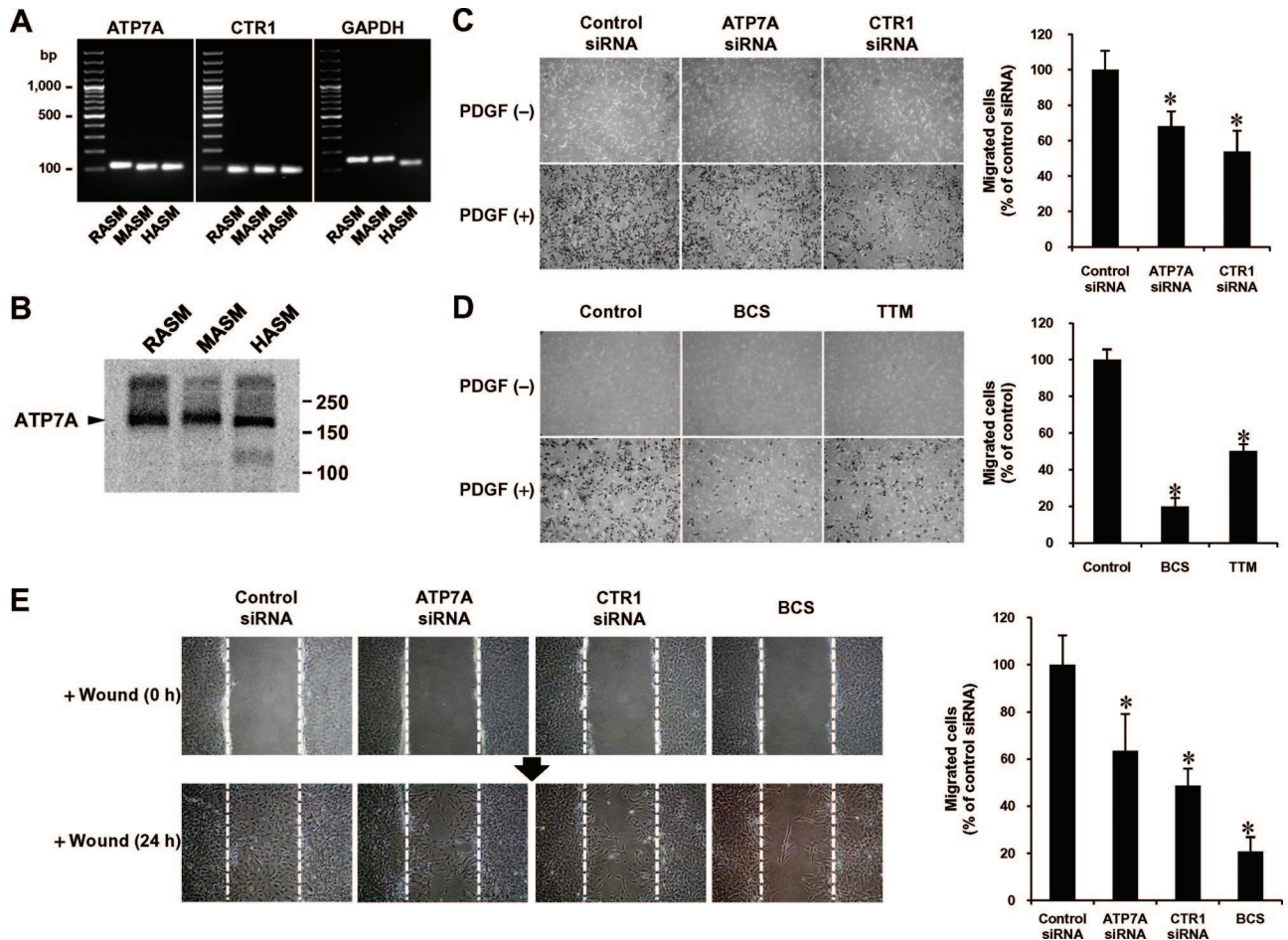


**Figure 1. ATP7A is involved in VSMC migration stimulated by PDGF or wound scratch in a copper-dependent manner.** **A**, RT-PCR analysis of ATP7A and CTR1 mRNA expression in various VSMCs (RASMs, HASMs, and MASMs). **B**, Western blot analysis of ATP7A protein expression in various VSMCs. **C and D**, RASMs were transfected with ATP7A, CTR1, or control siRNA for 48 hours or treated with the copper chelator BCS (cell-impermeable) (200  $\mu$ mol/L for 72 hours) or the copper chelator TTM (cell-permeable) (10 nmol/L for 24 hours). Cell migration was assessed by the modified Boyden chamber assay after stimulation with or without 50 ng/mL PDGF for 8 hours. **E**, Wound-scratch assay was performed in confluent monolayers of RASMs transfected with siRNA or treated with copper chelator in the presence of PDGF (50 ng/mL), as described in the Online Data Supplement. Images were captured immediately after rinsing at 0 hour and at 24 hours after the wounding in the cells. **Bar graph** represents averaged data, expressed as cell number per field. \* $P < 0.05$  vs control siRNA-treated (**C and E**) or untreated (**D and E**) cells. Values are the means  $\pm$  SD for 3 independent experiments.

copper transporter function of ATP7A is dependent on the delivery of copper from the extracellular space via CTR1,<sup>29,30</sup> we also investigated the role of CTR1. Transfection of VSMCs with CTR1 siRNA significantly reduced endogenous CTR1 expression (Online Figures I [A] and V [B]). PDGF-induced cell migration was significantly inhibited by CTR1 siRNA (Figure 1C) as well as copper chelators tetrathiomolybdate (TTM) (cell-permeable) and bathocuproine disulfonate (BCS) (cell-impermeable) (Figure 1D), suggesting that this response is copper-dependent. Wound scratch assay of confluent monolayer of VSMCs in the presence of PDGF also showed that ATP7A siRNA as well as CTR1 siRNA or BCS significantly inhibited directional cell migration in response to wound injury (Figure 1E). In contrast, transfection of ATP7A siRNA did not have significant effect on PDGF-induced VSMC proliferation (Online Figure II). These results suggest that ATP7A is involved in PDGF-stimulated VSMCs migration in a copper-dependent manner.

### PDGF Stimulation Promotes ATP7A Translocation to the Leading Edge in a Copper-Dependent Manner

To gain insight into the mechanism by which ATP7A mediates VSMC migration in response to PDGF, we examined the subcellular localization of ATP7A after wound scratch in the presence of PDGF. In confluent monolayers of VSMC before wounding or in migrating VSMCs away from the scratched area, ATP7A was found predominantly in perinuclear regions (Figure 2A). In contrast, ATP7A accumulated and colocalized with F-actin at the leading edge in actively migrating VSMCs, but did not colocalize with actin stress fibers in the cell body (Figure 2A). We confirmed the specificity of the ATP7A staining by ATP7A siRNA, as shown later (Figure 3D). Furthermore, nonimmune IgG (control) showed no staining (data not shown). Pretreatment of VSMCs with copper chelators BCS or TTM as well as CTR1 siRNA markedly inhibited wound-induced transloca-

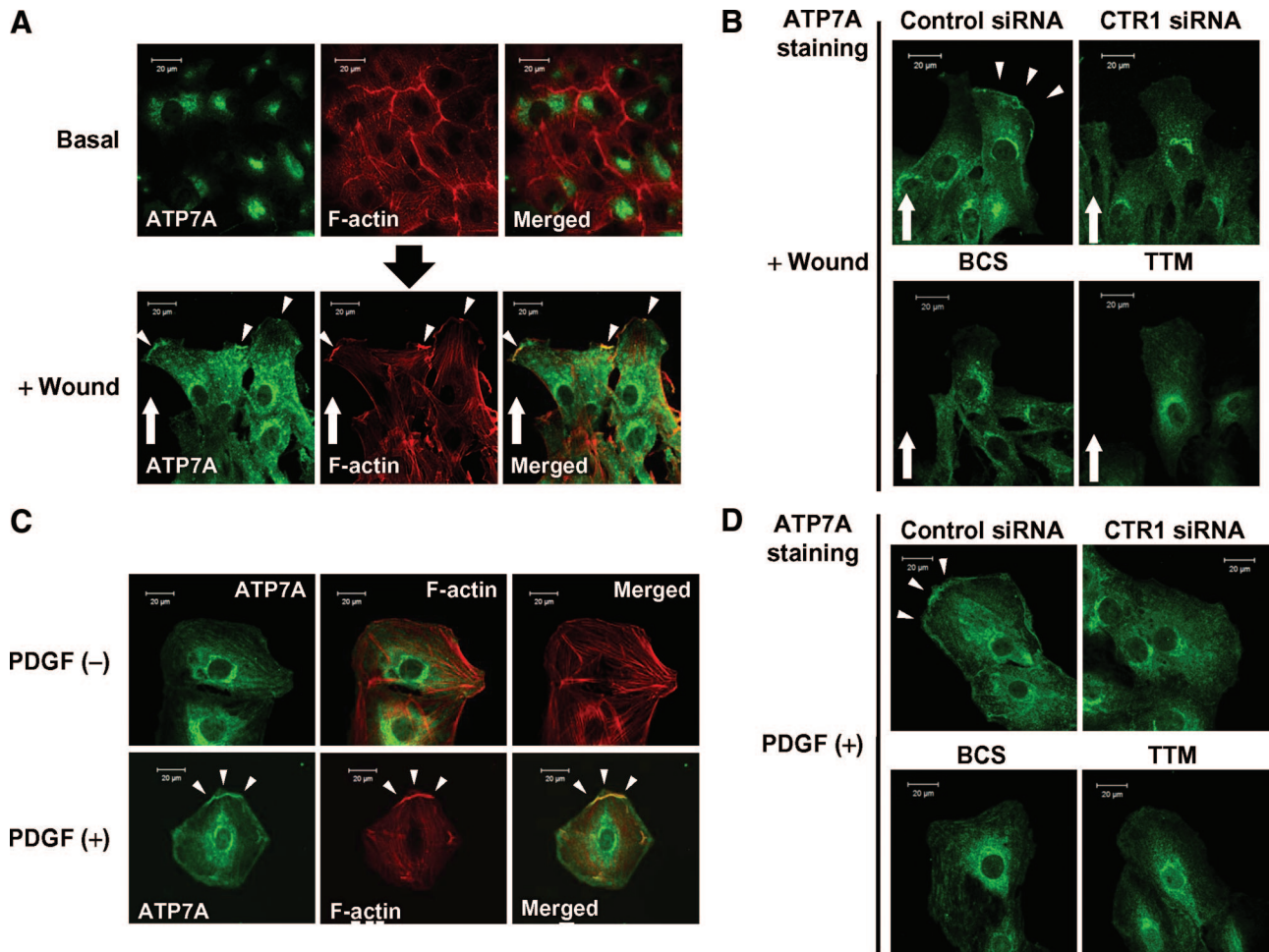


**Figure 2. ATP7A is translocated to the leading edge in VSMCs stimulated by wound scratch or PDGF in a copper-dependent manner.** **A and B**, Confluent monolayer of RASMs before (**top**) and after wound scratch in the presence of 50 ng/mL PDGF for 18 hours (**bottom**) were stained with anti-ATP7A (**green**) and Alexa Fluor 568-phalloidin (**red**) antibodies. **Small white arrowheads** point to the leading edge, and **large arrows** point to direction of migration. **C and D**, Growth-arrested RASMs were stimulated with or without 50 ng/mL PDGF for 5 minutes. Cells were costained for ATP7A and phalloidin. In some experiments, RASMs transfected with CTR1, or control siRNA, or treated with copper chelators BCS or TTM were stimulated by wound scratch (**B**) or PDGF (**D**). Results for **A through D** are representative of 3 independent replicates of immunofluorescence images.

tion of ATP7A toward the leading edge (Figure 2B). Similarly, in untreated VSMC, ATP7A was found predominantly in perinuclear regions, and colocalized with syntaxin 6, a TGN marker (Online Figure III, B). PDGF stimulation rapidly promoted ATP7A translocation from the Golgi to the plasma membrane leading edge with peak at 5 minutes, which gradually returned to the perinuclear region within 30 minutes (Figure 2C; Online Figure III, A). This effect was observed in VSMCs from other species, such as MASMs, suggesting that function of ATP7A is similar in VSMC across the different species (Online Figure III, C). Furthermore, this response was inhibited by copper chelators as well as knock-down of CTR1 (Figure 2D). Of note, the location of syntaxin 6 was not altered by PDGF in VSMCs (Online Figure III, B), suggesting that PDGF-induced ATP7A translocation was not attributable to the general effect on Golgi structure. Taken together, these findings suggest that PDGF stimulation promotes ATP7A translocation to the leading edge, in a copper-dependent manner, thereby stimulating VSMC migration.

#### ATP7A Is Involved in PDGF-Stimulated Lamellipodia Formation and Rac1 Translocation in a CTR1-Dependent Manner in VSMCs

To assess further the mechanism by which ATP7A is involved in VSMC migration, we examined whether ATP7A is involved in actin reorganization. Knockdown of ATP7A by siRNA significantly impaired wound scratch- (Figure 3A) and PDGF- (Figure 3B) stimulated lamellipodia formation at the leading edge in VSMCs as visualized by phalloidin staining. These effects were also prevented by siRNA knock-down of the CTR1. Because Rac1 plays a role in lamellipodia formation and cell migration,<sup>31</sup> we next examined the role of ATP7A in Rac1 activation and translocation in PDGF-stimulated VSMCs. PDGF stimulation increased active, GTP-bound form of Rac1 within 1 minute, which was not affected by either ATP7A or CTR1 siRNA (Online Figure IV). Immunofluorescence analysis showed that PDGF stimulation promoted translocation of Rac1 to the leading edge where it colocalized with ATP7A (Figure 3C). Coimmuno-

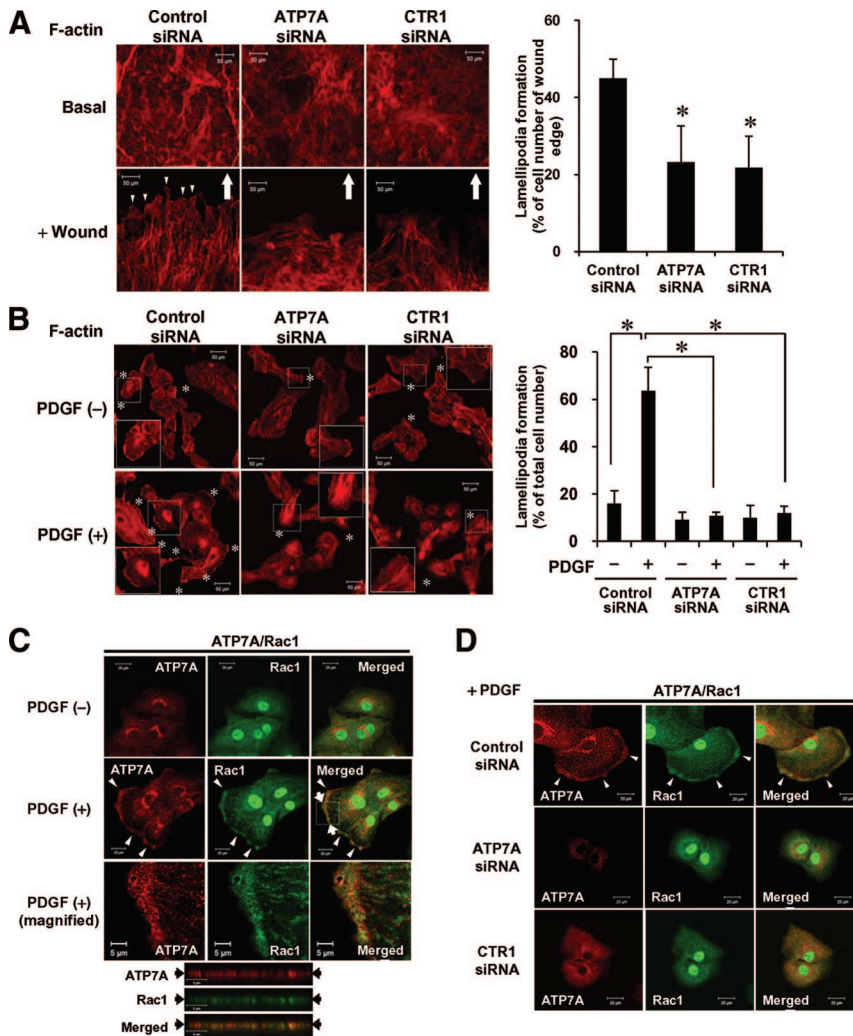


**Figure 3. ATP7A is involved in PDGF-stimulated lamellipodia formation and Rac1 translocation in a CTR1-dependent manner in VSMCs.** **A** and **B**, RASMs transfected with control siRNA or CTR1 siRNA or ATP7A siRNA were stimulated with wound scratch (**A**) or 50 ng/mL PDGF (**B**) as described for Figure 2, and cells were stained for phalloidin to visualize lamellipodia formation. Cells with lamellipodia formation were expressed as percentage of cell number of wound edge (**A**) or total cell number (**B**) (means  $\pm$ SD,  $n=3$ ). In **B**, cells in boxes are magnified in insets. Small white arrowheads point to the leading edge, and large black arrows point to direction of migration. \* $P<0.05$  vs control siRNA-treated cells. **C** and **D**, RASMs stimulated with or without PDGF as described above and costained with anti-ATP7A antibody (red) and anti-Rac1 antibody (green). In **D**, RASMs were transfected with control siRNA or CTR1 siRNA or ATP7A siRNA as described. All fluorescence images were taken at 5 different fields/well, and the cell images are representative of  $>3$  different experiments.

precipitation analysis showed that ATP7A associated with Rac1 in the basal state, which was further enhanced after PDGF stimulation (Online Figure IV, C), suggesting that ATP7A recruits Rac1 to the lipid rafts via binding to Rac1 in response to PDGF directly or indirectly. Furthermore, Rac1 trafficking to the leading edge was inhibited by either ATP7A or CTR1 siRNA (Figure 3D). Thus, the copper transporter ATP7A is involved in PDGF-stimulated translocation of Rac1 to the leading edge, but not Rac1 activation, in a CTR1-dependent manner, which may contribute to lamellipodia formation and VSMC migration.

### ATP7A Colocalizes With PDGFR at the Leading Edge in a CTR1-Dependent Manner in PDGF-Stimulated VSMCs

Because we found that ATP7A is a downstream mediator for PDGFR signaling linked to VSMC migration, we next examined the relationship between ATP7A and PDGFR in PDGF-stimulated VSMCs. Immunofluorescence analysis showed that ATP7A colocalized with PDGFR at the leading edge after PDGF stimulation (Figure 4A). Of note, both CTR1 and ATP7A siRNAs inhibited PDGF-induced ATP7A movement to the leading edge without affecting PDGFR localization (Figure 4B). Coimmunoprecipitation analysis

further confirmed that PDGF stimulation promoted PDGFR association with ATP7A, which was somewhat inhibited by CTR1 siRNA (Figure 4C). Under this condition, PDGF-induced PDGFR autophosphorylation was not affected by CTR1 siRNA (Figure 4C). Taken together, these results suggest that PDGF stimulation induces colocalization and association of ATP7A with PDGFR at the leading edge in a CTR1-dependent manner, and that CTR1-ATP7A pathway is downstream of PDGFR activation.

### PDGF Promotes ATP7A Recruitment to the Caveolae/Lipid Rafts, Where PDGFR, Rac1, and CTR1 Are Localized, in a CTR1-Dependent Manner

To gain further insight into the subcellular compartments in which ATP7A is localized, we performed detergent-free sucrose gradient fractionation in VSMCs, as previously described.<sup>32</sup> Western analysis of sequential fractions from the gradient showed that ATP7A was found in both caveolin-enriched lipid rafts fractions and noncaveolae/lipid rafts fractions which mainly contain paxillin (Figure 5A).<sup>33</sup> By contrast, the CTR1 copper importer was predominantly found in caveolae/lipid rafts. The specificity of the CTR1 antibody, which detects glycosylated CTR1,<sup>34</sup> was verified by CTR1-deficient mouse embryonic fibroblast cells<sup>30</sup> and VSMCs

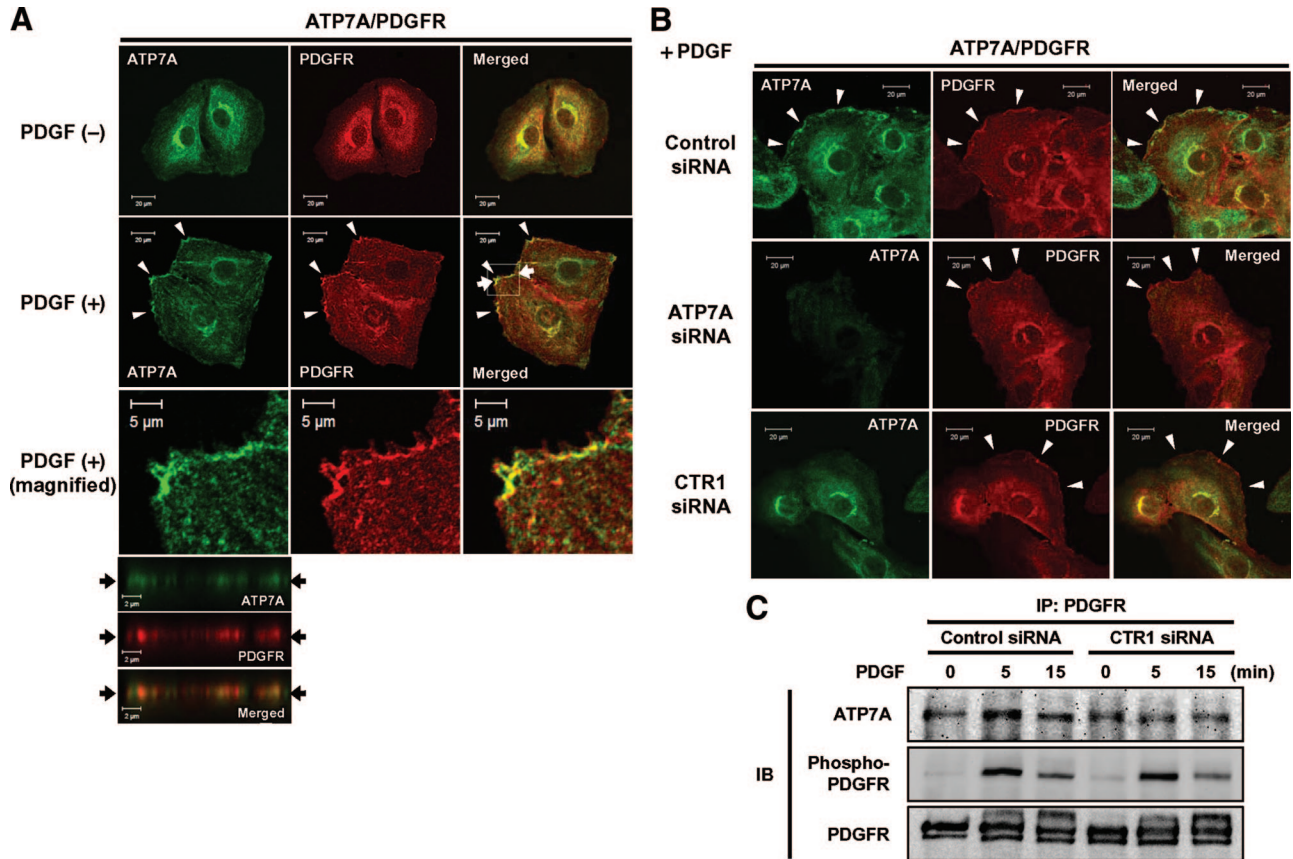


**Figure 4. ATP7A colocalizes with PDGFR at the leading edge in a CTR1-dependent manner in PDGF-stimulated VSMCs. A through C,** Growth-arrested RASMs were stimulated with 50 ng/mL PDGF for 5 minutes. All fluorescence images were taken at 5 different fields/well, and the cell images are representative of >3 different experiments. **A,** Effect of PDGF on subcellular localization of ATP7A and PDGFR in VSMCs. RASMs were stained with anti-ATP7A antibody (green) and anti-PDGFR antibody (red). **B,** Effect of ATP7A or CTR1 siRNA on subcellular localization of ATP7A and PDGFR in PDGF-treated cells. RASMs transfected with CTR1, ATP7A, or control siRNA were double-stained with anti-ATP7A antibody (green) and anti-PDGFR antibody (red). **C,** PDGF stimulation promoted PDGFR association with ATP7A in a CTR1-dependent manner. RASMs were transfected with control siRNA or CTR1 siRNA. Growth-arrested confluent monolayer of RASMs was stimulated with 50 ng/mL PDGF for indicated times (min). Lysates were immunoprecipitate (IP) with anti-PDGFR antibody, followed by immunoblot (IB) with ATP7A, phospho-PDGFR, and PDGFR antibody.

transfected with CTR1 siRNA (Online Figure V, A and B). Localization of ATP7A and CTR1 in caveolae/lipid rafts was further confirmed in various VSMCs, including RASM, HASM, and MASM (Online Figure V, C) and using detergent-free OptiPrep gradient cell fractionation (Online Figure V, D). Figure 5B shows that PDGF stimulation for 5 minutes promoted recruitment of ATP7A, CTR1 and Rac1 to the caveolae/lipid rafts fractions without affecting PDGFR localization, which was associated with an increase in PDGFR phosphorylation in these fractions. Significantly, CTR1 siRNA prevented PDGF-induced translocation of ATP7A and Rac1 to the caveolae/lipid rafts without affecting PDGFR phosphorylation (Figure 5B). These results suggest that PDGF-induced PDGFR autophosphorylation occurs in caveolae/lipid rafts, which in turn promotes recruitment of ATP7A and Rac1 to these specialized microdomains where PDGFR is localized, in a CTR1-dependent manner.

#### ATP7A Is Translocated to the Lipid Rafts Localized at the Leading Edge in PDGF-Stimulated VSMCs

Lipid rafts have been shown to be localized at the leading edge during cell migration.<sup>35</sup> We thus examined the spatial

relationships among ATP7A, lipid rafts and leading edge after PDGF stimulation using immunofluorescence analysis. As shown in Figure 5C and Online Figure VI (B), ATP7A colocalized with cholera toxin subunit B (CTxB), a lipid raft marker,<sup>35</sup> at the leading edge in PDGF- and wound scratch-stimulated VSMCs. Furthermore, CTxB accumulated and colocalized with F-actin at the leading edge in actively migrating VSMCs (Online Figure VI, A and C). Disruption of lipid rafts by cholesterol binding reagent, methyl- $\beta$ -cyclodextrin, completely abrogated the ATP7A localization at the leading edge and CTxB staining (Figure 5D) as well as lamellipodia formation (Online Figure VI, A). These results suggest that PDGF stimulates translocation of ATP7A to the lipid rafts localized at the leading edge, thereby promoting lamellipodia formation.

#### PDGF Stimulation Reduces Copper Content in Caveolae/Lipid Raft Fractions in VSMCs

Because ATP7A is involved in exporting copper to the extracellular space, we next examined the effects of PDGF on copper levels in VSMCs. At first, we performed <sup>64</sup>Cu



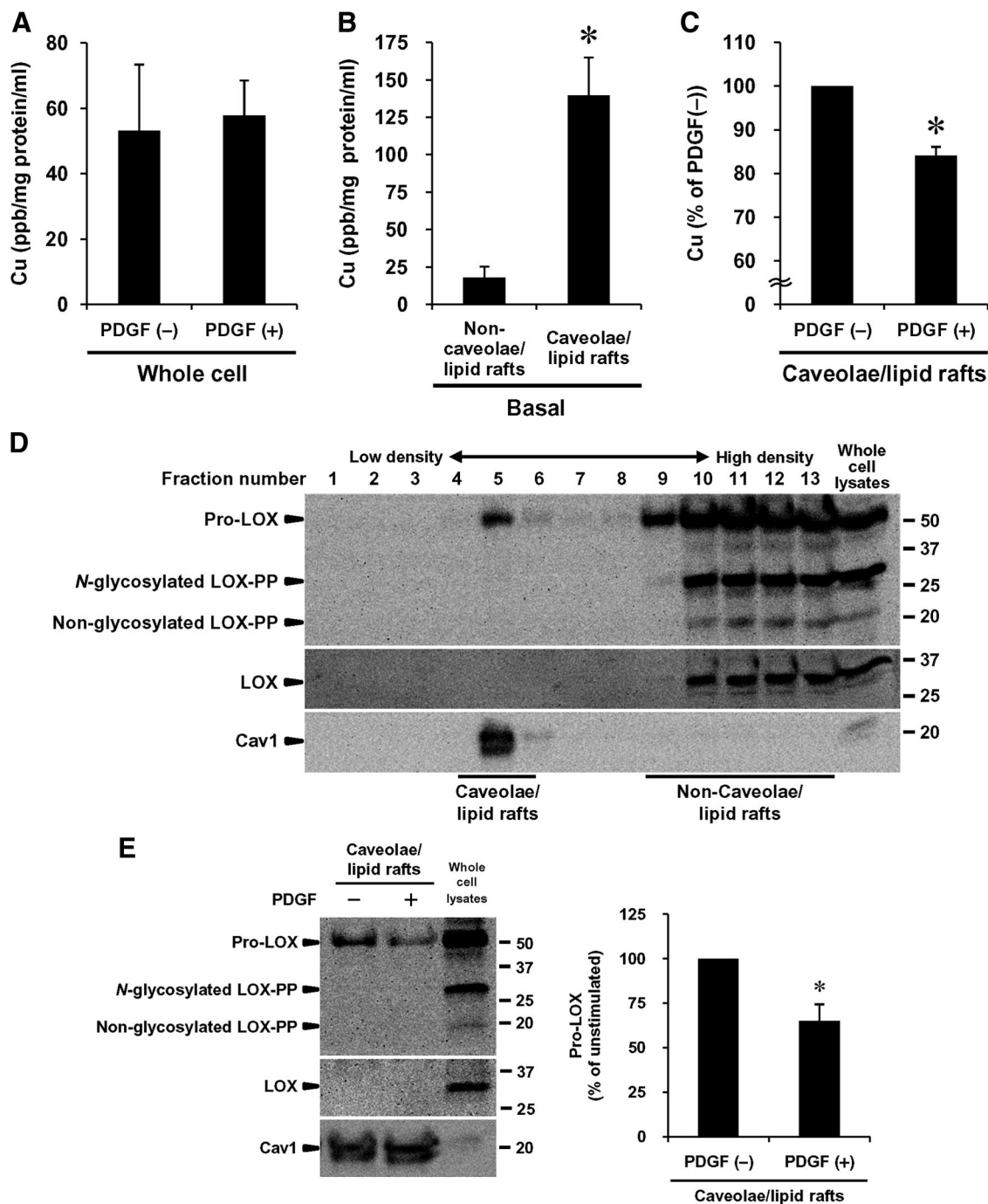


**Figure 6. PDGF stimulation reduces copper content and Pro-LOX in lipid rafts fractions in VSMCs.** **A through C**, Copper contents were measured by ICP-MS in whole cells (**A**) or caveolae/lipid rafts or noncaveolae/lipid rafts (**B and C**) in RASMs with or without PDGF stimulation for 5 minutes. Equal amounts of proteins in caveolae/lipid rafts (fractions 4 to 5) or noncaveolae/lipid rafts (fractions 9 to 13) were obtained by sucrose gradient fractionation as described for Figure 5. \* $P < 0.05$  vs nonlipid rafts or unstimulated cells (means  $\pm$  SD,  $n = 3$ ). **D**, Identification of Pro-LOX, but not LOX, in caveolae/lipid rafts in VSMCs. RASMs were fractionated by sucrose gradient centrifugation, followed by immunoblotted with anti-LOX-PP (which detects both Pro-Lox and LOX-PP), anti-LOX, or anti-caveolin-1 antibodies. **E**, Effect of PDGF treatment on Pro-LOX level in caveolae/lipid rafts fractions in VSMCs. Equal amounts of proteins in caveolae/lipid rafts (fractions 4 to 5) were immunoblotted with anti-LOX-PP, -LOX, or -caveolin-1 antibodies in RASMs with or without 50 ng/mL PDGF for 5 minutes.

itrite (BAPN), significantly inhibits PDGF-induced VSMC migration (Online Figure XII, B), which is consistent with the report by Lucero et al.<sup>24</sup> These findings suggest that LOX activity is involved in PDGF-induced, ATP7A-dependent VSMC migration.

### ATP7A Is Upregulated in Neointimal Formation in Response to Vascular Injury In Vivo

To determine the functional significance of ATP7A in VSMC migration in vivo, we examined the role of ATP7A in neointimal formation using a mouse wire injury model.

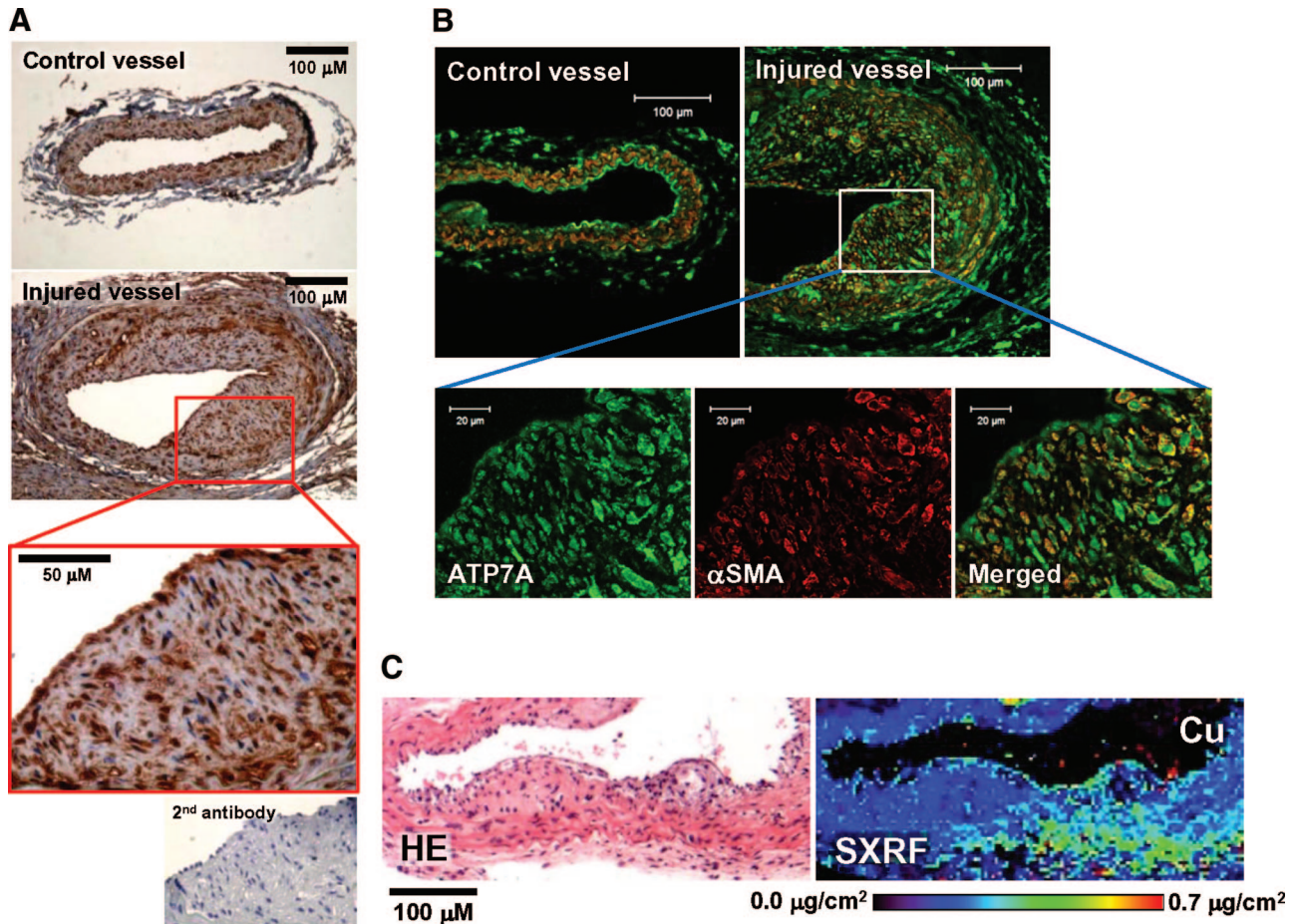


**Figure 7. ATP7A is involved in neointimal formation in response to vascular injury in vivo.** **A** and **B**, ATP7A is highly expressed in neointimal VSMCs of wire-injured carotid arteries of ApoE-deficient atherosclerotic mice. Immunohistochemical (**A**) or immunofluorescence (**B**) analysis for uninjured (control) or injured (4 weeks after) carotid artery stained with anti-ATP7A antibody (**A**); or costained with anti-ATP7A (**green**) and  $\alpha$ -smooth muscle actin (**red**) antibodies (**B**). **C**, X-ray fluorescence microscopy scans of the neointima of wire-injured carotid arteries. Areas of neointimal lesions were identified by hematoxylin/eosin staining (**left**). X-ray fluorescence microscopy scans (1 to 2 seconds per pixel) were performed in paraffin-embedded tissue (**right**). Map of Cu shows areas of the lowest to the highest content scaled to a rainbow color (**bottom**). Copper accumulation in neointimal lesions is shown in **white arrow**. The minimal and maximal Cu content displayed in micrograms per square centimeter is shown in the image.

Immunohistochemical analysis showed that ATP7A protein expression was robustly increased in neointimal VSMC and endothelial cells lining the lumen in the injured vessel of ApoE-deficient atherosclerotic mice (Figure 7A). Immunofluorescence analysis demonstrated that ATP7A was colocalized with  $\alpha$ -smooth muscle actin, a VSMC marker, in the neointima formed in response to injury (Figure 7B). We next examined if induction of ATP7A precedes VSMC migration after injury to address the cause-effect of ATP7A in VSMC migration in vivo. As shown in Online Figure XI, we observed increase in ATP7A expression at 3 days after wire injury in the vessels of ApoE-deficient atherosclerotic mice, whereas there was no VSMC migration and neointima formation at this time point as reported by Linder et al.<sup>37</sup> Thus, these findings suggest that ATP7A expression is increased before the onset of VSMC migration following vascular injury and this upregulation is also observed in neointimal VSMCs. Finally, we examined spatial distribution of copper in neointima using synchrotron-based x-ray fluorescence microscopy (SXFM).<sup>28</sup> As shown in Figure 7C, copper accumulation was observed at neointimal lesions in wire

injury model. These results suggest that ATP7A may be involved in neointima formation in response to vascular injury in vivo.

## Discussion

A role for copper in tissue repair, neointima thickening and atherosclerosis has been suggested; however, the underlying detailed mechanisms remain unknown.<sup>3-7,9-11</sup> Here we provide novel evidence that the ATP7A copper transporter is involved in PDGF-stimulated VSMC migration, which is critical for neointimal formation and vascular remodeling (Figure 8). We found that stimulation with PDGF promotes ATP7A translocation from TGN to the leading edge. This PDGF-induced ATP7A movement toward the site of actin remodeling is inhibited by cell permeable and impermeable copper chelators as well as depletion of the CTR1 copper importer. It has been shown that relocalization of ATP7A from the Golgi is triggered by increased cytoplasmic copper as well as by estrogen, insulin, NMDA (*N*-methyl-D-aspartate) activation, hypoxia, and cytokines.<sup>2,16,38,39</sup> However, our data are the first demonstration that the ATP7A

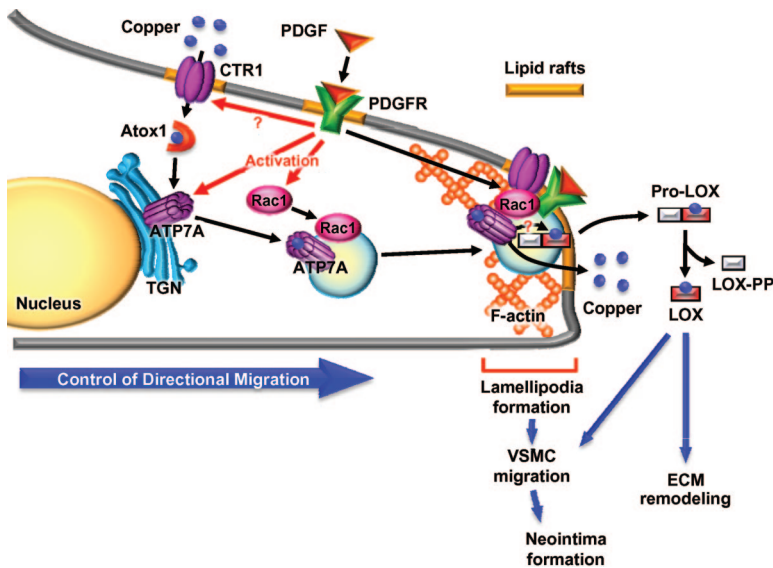


**Figure 8. Proposed model for role of ATP7A in PDGF-induced VSMC migration.** PDGF promotes ATP7A translocation from the TGN to the lipid rafts, which localize at the leading edge, thereby stimulating lamellipodia formation via recruiting Rac1, which in turn promotes directional VSMC migration involved in neointimal formation. This is associated with a decrease in cellular copper level and secretory copper enzyme prolysin oxidase (Pro-LOX) at the lipid rafts, which is extracellularly processed and activated by proteolysis to a mature lysyl oxidase (LOX-PP), which may promote extracellular matrix (ECM) remodeling and VSMC migration. Secreted copper may also contribute to PDGF-induced cell migration.

copper transporter translocates to the leading edge during growth factor-stimulated cell migration. It has been reported that ATP7A trafficking is in part dependent on its catalytic activity, which requires copper binding to conserved cysteines within its N-terminal region.<sup>17–19</sup> Extracellular copper influx is mainly mediated through CTR1, the copper importer, which is also the major source of “bioavailable” copper for ATP7A via the Atox1 copper chaperone.<sup>29,30</sup> Indeed, Atox1 siRNA prevented PDGF induced ATP7A translocation to the leading edge, suggesting that Atox1 is involved in PDGF-induced translocation of ATP7A (data not shown). Thus, our findings are consistent with the possibility that ATP7A obtains copper via Atox1 by stimulating extracellular copper uptake through CTR1 in response to PDGF, thereby promoting ATP7A trafficking from the Golgi to the leading edge in VSMCs. However, we failed to detect a PDGF-induced increase in <sup>64</sup>Cu uptake in whole cell labeling of VSMCs with <sup>64</sup>Cu in this study. This may be attributable to the possibility that CTR1-mediated copper uptake occurs in the specific plasma membrane compartment, as discussed below. It is not known how ATP7A is translocated to the leading edge after PDGF stimulation in a copper-dependent manner. Phosphorylation of ATP7A has been shown to be involved in copper-induced relocalization of this protein.<sup>40</sup> Thus, it is possible that PDGF stimulation may induce phosphorylation of ATP7A, which may contribute to its translocation to the leading edge. Taken together, our findings provide a novel linkage between copper homeostasis and PDGF-induced VSMC migration.

Migrating cells form protrusions, such as lamellipodia, by reorganizing of the actin cytoskeleton at the leading edge, which plays an important role in cell migration. The small G protein family Rac1 plays a key role in lamellipodia formation<sup>31</sup> and PDGF-stimulated cell migration.<sup>13</sup> In the present study, we demonstrate that ATP7A is involved in PDGF-induced lamellipodia formation and Rac1 translocation to the leading edge without affecting Rac1 activity, in a copper- and CTR1-dependent manner. Coimmunoprecipitation analysis showed that ATP7A as-

sociated with Rac1 in the basal state, which was further enhanced after PDGF stimulation (Online Figure IV, C), suggesting that ATP7A recruits Rac1 to the lipid rafts via binding to Rac1 in response to PDGF directly or indirectly. In line with our data, previous reports show that trafficking of ATP7A from the TGN to the cell surface is associated with actin networks and involves Rac1, which is distinct from the major constitutive secretory pathway.<sup>16,41</sup> Of note, PDGF stimulation also promotes colocalization and association of ATP7A with PDGFR at the leading edge. However, CTR1 siRNA prevents ATP7A translocation to the leading edge without affecting PDGFR localization and its autophosphorylation. These results suggest that CTR1-ATP7A-Rac1 pathway is downstream of PDGFR activation involved in lamellipodia formation and VSMC migration.

Caveolae and lipid rafts are specialized membrane microdomains that are highly enriched in cholesterol and sphingolipids and function as platforms for assembly of signaling molecules including G proteins and receptors involved in various functions.<sup>35</sup> In chemoattractant-stimulated cancer cells, lipid rafts are accumulated at the leading edge.<sup>35</sup> Using sucrose gradient fractionation, the present study shows that PDGF stimulation promotes recruitment of ATP7A and Rac1 to the caveolae/lipid rafts where CTR1 and PDGFR are localized, in a CTR1-dependent manner. By contrast, CTR1 siRNA has no effect on PDGF-induced PDGFR tyrosine phosphorylation as well as localization of caveolin-1 and PDGFR in caveolae/lipid rafts fractions, suggesting that the structure of caveolae/lipid rafts is intact in CTR1 depleted VSMCs. Immunofluorescence analysis also reveals that the marker for lipid rafts, CTxB,<sup>35</sup> colocalizes with ATP7A at the leading edge of migrating VSMCs. We confirmed the plasma membrane localization of ATP7A and CTR1 in PDGF-stimulated VSMCs using cell surface biotinylation assays. PDGF-induced Rac1 translocation to the lipid rafts has been reported in Rat-1B cells<sup>13</sup>; however, our data provides the first evidence that copper transporters CTR1 and ATP7A are localized in these specialized plasma membrane microdo-

mains. Functional significance of copper-dependent ATP7A trafficking into lipid rafts is demonstrated by showing that disruption of lipid rafts by the cholesterol-binding reagent, methyl- $\beta$ -cyclodextrin, completely inhibits PDGF-induced ATP7A translocation to the leading edge as well as lamellipodia formation. Moreover, PDGF stimulation rapidly decreases the copper content of caveolae/lipid rafts in an ATP7A-dependent manner, as measured by ICP-MS. This PDGF effect is associated with recruitment of ATP7A to lipid rafts where CTR1 is predominantly found. The rapid kinetics of ATP7A is reminiscent of copper-induced ATP7A recruitment into a fast-recycling pool located in close proximity with the plasma membrane.<sup>2,16,17,42</sup> Hung YH et al have reported that the copper content of lipid rafts is paradoxically decreased, when cytoplasmic copper is increased.<sup>43</sup> Thus, it is conceivable that PDGF may stimulate copper uptake via CTR1 to provide copper to ATP7A, which in turn promotes ATP7A translocation from the Golgi to the caveolae/lipid rafts to export copper to extracellular space in the specific compartments. Interestingly, we could not detect any changes in copper levels in response to PDGF in total cell lysates. This may support the suggestion that global measurements of <sup>64</sup>Cu efflux and <sup>64</sup>Cu uptake in whole cells would fail to detect compartmentalized changes of copper distribution observed in the present study.

The physiological consequence of copper export via ATP7A is not merely the elimination of excess cellular copper, but to supply adequate copper to the developing fetus as gestation progresses,<sup>16</sup> or to provide copper as part of a neuronal protective mechanism.<sup>2</sup> Using SXFM, Finney et al reported that copper is transported from intracellular compartments to the tips of endothelia during capillary growth, which is required for capillary tube formation.<sup>28</sup> In the present study, we demonstrate that the copper-dependent Pro-LOX, which is secreted and activated in the extracellular space,<sup>22</sup> is localized at caveolae/lipid rafts in the basal state. PDGF stimulation significantly reduces Pro-LOX levels in caveolae/lipid rafts fractions in an ATP7A-dependent manner. This may reflect the secretion of pro-LOX after obtaining copper from the recruited ATP7A in these specialized compartments. Importantly, recent evidence suggests that LOX and LOX-PP, both of which are produced from Pro-LOX through proteolysis in the extracellular space, have opposite effects on cell migration.<sup>23–25</sup> Furthermore, and consistent with our results, ATP7A has been shown to deliver copper to some secretory copper enzymes in the post-Golgi vesicles rather than in the TGN, where copper loading normally takes place.<sup>38,44</sup> Taken together, these findings suggest that copper-dependent ATP7A trafficking to lipid rafts in response to PDGF may not simply reflect export copper to the extracellular space, but also facilitate copper-loading to pro-LOX in post-Golgi compartments such as lipid rafts, thereby promoting VSMC migration. To support this, we found that ATP7A siRNA significantly inhibited LOX activity in VSMCs treated with PDGF and that the chemical LOX activity inhibitor  $\beta$ -aminopropionitrile significantly blocked PDGF-induced VSMC migration.

A functional role of the copper transporter ATP7A in VSMC migration in vivo is underscored by upregulation of ATP7A expression and copper accumulation (shown by SXFM) in intimal a-smooth muscle actin positive cells. Of note, ATP7A expression is increased before the onset of VSMC migration after vascular injury and this upregulation was also observed in neointimal VSMCs at later time. These findings suggest that ATP7A may play a role in VSMC migration in vivo. Previous reports indicate that copper plays an important role in various cardiovascular diseases and cancer. High serum copper levels are associated with an increased future risk of coronary heart disease.<sup>4,5,7</sup> Atherosclerotic lesions have higher copper levels than normal tissues.<sup>9</sup> Neointimal thickening after vascular injury is inhibited by copper chelation<sup>11</sup> and increased by copper cuffs and stents.<sup>10</sup> Copper deficiency therapies prevent tumor progression in clinical trials.<sup>3</sup> Interestingly, we found that ATP7A is involved in PDGF-stimulated decrease in copper level and Pro-LOX in caveolae/lipid rafts as well as PDGF-stimulated increase in LOX activity in VSMCs. Furthermore, we showed that inhibition of LOX activity blocks PDGF-induced VSMC migration as reported previously.<sup>24</sup> Given that LOX activity is also essential for vascular extracellular matrix maturation, these results suggest that ATP7A copper transporter may promote extracellular matrix deposition, as well as neointimal formation after vascular injury via regulation of LOX activity.<sup>45</sup> In addition, one of the major copper- and ATP7A-dependent enzymes regulating ROS metabolism is SOD3, but not either SOD1 or SOD2.<sup>21</sup> We thus investigated the contribution of SOD3 but found that SOD3 siRNA had no effect of PDGF-induced directional VSMC migration (Online Figure XII, C). X-ray fluorescence microscopy scans do not clearly show codistribution of copper levels with ATP7A. This may be attributable to the possibility that copper secreted by ATP7A is more widely distributed because of the diffusible nature as ions, and that other copper binding proteins may be involved in neointima formation. Taken together with in vitro data, our findings indicate that upregulation of ATP7A and copper accumulation in neointimal VSMCs may contribute to neointimal formation and vascular remodeling in vivo at least in part by regulating VSMC migration and LOX activity. Because our vascular injury data implicates but does not conclude that ATP7A may play a role in VSMC migration in vivo, further investigation will be required using ATP7A mutant mice<sup>46</sup> in future study.

In conclusion, the present study uncovers a novel function of ATP7A as a regulator for PDGF-induced VSMC migration via recruiting Rac1 to lipid rafts at the leading edge in a copper dependent manner, as well as controlling LOX activity, which may contribute to vascular remodeling (Figure 8). They also indicate an important new role for lipid rafts in organizing the protein components involved in copper homeostasis and signaling. Our findings also provide insight into ATP7A as a potential therapeutic target for various pathophysiologicals, such as atherosclerosis, postangioplasty restenosis, diabetes, and cancer, which are associated with dysregulation of cell migration.

## Acknowledgments

We thank Dr Dennis Thiele (Duke University, Durham, NC) for the generous gift of CTR1<sup>-/-</sup> and CTR1<sup>+/+</sup> mouse embryonic fibroblasts.

## Sources of Funding

This work was supported by NIH grants R01 HL070187 (T.F.), R01 HL077524 (to M.U.-F.), and R01 HL080569-01 (to Y.H.); American Heart Association Postdoctoral Fellowship 09POST2250151 (to N.U.); Ruth L. Kirschstein-National Service Research Award (Kirschstein-NRSA) T32 training grant (to G-F.C.); the Uehara Memorial Foundation (to J.O.); the Naito Foundation (to J.O.); American Diabetes Association Research Award 1-10-BS-76 (to Y.H.); and American Heart Association Grant 10GRNT4400005 (to Y.H.). Use of the Advanced Photon Source at Argonne National Laboratory was supported by the US Department of Energy, Office of Science, Office of Basic Energy Sciences, under contract no. DE-AC02-06CH11357.

## Disclosures

None.

## References

- Kim BE, Nevitt T, Thiele DJ. Mechanisms for copper acquisition, distribution and regulation. *Nat Chem Biol*. 2008;4:176–185.
- Schliet ML, Gitlin JD. Copper homeostasis in the CNS: a novel link between the NMDA receptor and copper homeostasis in the hippocampus. *Mol Neurobiol*. 2006;33:81–90.
- Brewer GJ. Anticopper therapy against cancer and diseases of inflammation and fibrosis. *Drug Discov Today*. 2005;10:1103–1109.
- Brewer GJ. Iron and copper toxicity in diseases of aging, particularly atherosclerosis and Alzheimer's disease. *Exp Biol Med (Maywood)*. 2007;232:323–335.
- Ferns GA, Lamb DJ, Taylor A. The possible role of copper ions in atherogenesis: the Blue Janus. *Atherosclerosis*. 1997;133:139–152.
- Saari JT, Schuschke DA. Cardiovascular effects of dietary copper deficiency. *Biofactors*. 1999;10:359–375.
- Klevay LM. Cardiovascular disease from copper deficiency—a history. *J Nutr*. 2000;130:489S–492S.
- Harris ED. A requirement for copper in angiogenesis. *Nutr Rev*. 2004;62:60–64.
- Stadler N, Lindner RA, Davies MJ. Direct detection and quantification of transition metal ions in human atherosclerotic plaques: evidence for the presence of elevated levels of iron and copper. *Arterioscler Thromb Vasc Biol*. 2004;24:949–954.
- Volker W, Dorszewski A, Unruh V, Robenek H, Breithardt G, Buddecke E. Copper-induced inflammatory reactions of rat carotid arteries mimic restenosis/arteriosclerosis-like neointima formation. *Atherosclerosis*. 1997;130:29–36.
- Mandinov L, Mandinova A, Kyurkchiev S, Kyurkchiev D, Kehayov I, Kolev V, Soldi R, Bagala C, de Muinck ED, Lindner V, Post MJ, Simons M, Bellum S, Prudovsky I, Maciag T. Copper chelation represses the vascular response to injury. *Proc Natl Acad Sci U S A*. 2003;100:6700–6705.
- Raines EW. PDGF and cardiovascular disease. *Cytokine Growth Factor Rev*. 2004;15:237–254.
- Ronnstrand L, Heldin CH. Mechanisms of platelet-derived growth factor-induced chemotaxis. *Int J Cancer*. 2001;91:757–762.
- Rae TD, Schmidt PJ, Pufahl RA, Culotta VC, O'Halloran TV. Undetectable intracellular free copper: the requirement of a copper chaperone for superoxide dismutase. *Science*. 1999;284:805–808.
- Kaplan JH, Lutsenko S. Copper transport in mammalian cells: special care for a metal with special needs. *J Biol Chem*. 2009;284:25461–25465.
- La Fontaine S, Mercer JF. Trafficking of the copper-ATPases, ATP7A and ATP7B: role in copper homeostasis. *Arch Biochem Biophys*. 2007;463:149–167.
- Lutsenko S, Barnes NL, Barteo MY, Dmitriev OY. Function and regulation of human copper-transporting ATPases. *Physiol Rev*. 2007;87:1011–1046.
- Petris MJ, Voskoboinik I, Cater M, Smith K, Kim BE, Llanos RM, Strausak D, Camakaris J, Mercer JF. Copper-regulated trafficking of the Menkes disease copper ATPase is associated with formation of a phosphorylated catalytic intermediate. *J Biol Chem*. 2002;277:46736–46742.
- Strausak D, La Fontaine S, Hill J, Firth SD, Lockhart PJ, Mercer JF. The role of GMXCXC metal binding sites in the copper-induced redistribution of the Menkes protein. *J Biol Chem*. 1999;274:11170–11177.
- Mercer JF. The molecular basis of copper-transport diseases. *Trends Mol Med*. 2001;7:64–69.
- Qin Z, Gongora MC, Ozumi K, Itoh S, Akram K, Ushio-Fukai M, Harrison DG, Fukai T. Role of Menkes ATPase in angiotensin II-induced hypertension: a key modulator for extracellular superoxide dismutase function. *Hypertension*. 2008;52:945–951.
- Payne SL, Hendrix MJ, Kirschmann DA. Paradoxical roles for lysyl oxidases in cancer—a prospect. *J Cell Biochem*. 2007;101:1338–1354.
- Hurtado PA, Vora S, Sume SS, Yang D, St Hilaire C, Guo Y, Palamankumbura AH, Schreiber BM, Ravid K, Trackman PC. Lysyl oxidase propeptide inhibits smooth muscle cell signaling and proliferation. *Biochem Biophys Res Commun*. 2008;366:156–161.
- Lucero HA, Ravid K, Grimsby JL, Rich CB, DiCamillo SJ, Maki JM, Myllyharju J, Kagan HM. Lysyl oxidase oxidizes cell membrane proteins and enhances the chemotactic response of vascular smooth muscle cells. *J Biol Chem*. 2008;283:24103–24117.
- Zhao Y, Min C, Vora SR, Trackman PC, Sonenshein GE, Kirsch KH. The lysyl oxidase attenuates fibronectin-mediated activation of focal adhesion kinase and p130Cas in breast cancer cells. *J Biol Chem*. 2009;284:1385–1393.
- Jeney V, Itoh S, Wendt M, Gradek Q, Ushio-Fukai M, Harrison DG, Fukai T. Role of antioxidant-1 in extracellular superoxide dismutase function and expression. *Circ Res*. 2005;96:723–729.
- Wang H, Zhang W, Tang R, Heibel RP, Kowalska MA, Zhang C, Marth JD, Fukuda M, Zhu C, Huo Y. Core2 1-6-N-glucosaminyltransferase-1 deficiency protects injured arteries from neointima formation in ApoE-deficient mice. *Arterioscler Thromb Vasc Biol*. 2009;29:1053–1059.
- Finney L, Mandava S, Ursos L, Zhang W, Rodi D, Vogt S, Legnini D, Maser J, Ikpat F, Olopade OI, Glesne D. X-ray fluorescence microscopy reveals large-scale relocalization and extracellular translocation of cellular copper during angiogenesis. *Proc Natl Acad Sci U S A*. 2007;104:2247–2252.
- Lin SJ, Pufahl RA, Dancis A, O'Halloran TV, Culotta VC. A role for the *Saccharomyces cerevisiae* ATX1 gene in copper trafficking and iron transport. *J Biol Chem*. 1997;272:9215–9220.
- Lee J, Petris MJ, Thiele DJ. Characterization of mouse embryonic cells deficient in the ctr1 high affinity copper transporter. Identification of a Ctr1-independent copper transport system. *J Biol Chem*. 2002;277:40253–40259.
- Ridley AJ. Rho GTPases and cell migration. *J Cell Sci*. 2001;114:2713–2722.
- Song KS, Li S, Okamoto T, Quilliam LA, Sargiacomo M, Lisanti MP. Co-purification and direct interaction of Ras with caveolin, an integral membrane protein of caveolae microdomains. Detergent-free purification of caveolae microdomains. *J Biol Chem*. 1996;271:9690–9697.
- Smart EJ, Ying YS, Mineo C, Anderson RG. A detergent-free method for purifying caveolae membrane from tissue culture cells. *Proc Natl Acad Sci U S A*. 1995;92:10104–10108.
- Maryon EB, Molloy SA, Kaplan JH. O-linked glycosylation at threonine 27 protects the copper transporter hCTR1 from proteolytic cleavage in mammalian cells. *J Biol Chem*. 2007;282:20376–20387.
- Manes S, Ana Lacalle R, Gomez-Mouton C, Martinez AC. From rafts to crafts: membrane asymmetry in moving cells. *Trends Immunol*. 2003;24:320–326.
- Peltonen L, Kuivaniemi H, Palotie A, Horn N, Kaitila I, Kivirikko KI. Alterations in copper and collagen metabolism in the Menkes syndrome and a new subtype of the Ehlers-Danlos syndrome. *Biochemistry*. 1983;22:6156–6163.
- Lindner V, Fingerle J, Reidy MA. Mouse model of arterial injury. *Circ Res*. 1993;73:792–796.
- White C, Kambe T, Fulcher YG, Sachdev SW, Bush AI, Fritsche K, Lee J, Quinn TP, Petris MJ. Copper transport into the secretory pathway is regulated by oxygen in macrophages. *J Cell Sci*. 2009;122:1315–1321.
- White C, Lee J, Kambe T, Fritsche K, Petris MJ. A role for the ATP7A copper-transporting ATPase in macrophage bactericidal activity. *J Biol Chem*. 2009;284:33949–33956.
- Veldhuis NA, Valova VA, Gaeth AP, Palstra N, Hannan KM, Michell BJ, Kelly LE, Jennings I, Kemp BE, Pearson RB, Robinson PJ, Camakaris J. Phosphorylation regulates copper-responsive trafficking of the Menkes

- copper transporting P-type ATPase. *Int J Biochem Cell Biol.* 2009;41:2403–2412.
41. Cobbold C, Coventry J, Ponnambalam S, Monaco AP. Actin and microtubule regulation of trans-Golgi network architecture, and copper-dependent protein transport to the cell surface. *Mol Membr Biol.* 2004;21:59–66.
  42. Pase L, Voskoboinik I, Greenough M, Camakaris J. Copper stimulates trafficking of a distinct pool of the Menkes copper ATPase (ATP7A) to the plasma membrane and diverts it into a rapid recycling pool. *Biochem J.* 2004;378:1031–1037.
  43. Hung YH, Robb EL, Volitakis I, Ho M, Evin G, Li QX, Culvenor JG, Masters CL, Cherny RA, Bush AI. Paradoxical condensation of copper with elevated beta-amyloid in lipid rafts under cellular copper deficiency conditions: implications for Alzheimer disease. *J Biol Chem.* 2009;284:21899–21907.
  44. Setty SR, Tenza D, Sviderskaya EV, Bennett DC, Raposo G, Marks MS. Cell-specific ATP7A transport sustains copper-dependent tyrosinase activity in melanosomes. *Nature.* 2008;454:1142–1146.
  45. Brasselet C, Durand E, Addad F, Al Haj Zen A, Smeets MB, Laurent-Maquin D, Bouthors S, Bellon G, de Kleijn D, Godeau G, Garnotel R, Gogly B, Lafont A. Collagen and elastin cross-linking: a mechanism of constrictive remodeling after arterial injury. *Am J Physiol Heart Circ Physiol.* 2005;289:H2228–H2233.
  46. Mercer JF. Menkes syndrome and animal models. *Am J Clin Nutr.* 1998;67:1022S–1028S.

## Novelty and Significance

### What Is Known?

- Copper is an essential micronutrient in all living organisms and involved in physiological repair processes, as well as various pathophysiologies including atherosclerosis.
- Copper deficiency therapies prevent neointimal thickening in response to vascular injury.
- Platelet-derived growth factor (PDGF) stimulates vascular smooth muscle cell (VSMC) migration, which promotes neointimal formation and vascular remodeling after vascular injury.

### What New Information Does This Article Contribute?

- Copper transporter ATP7A plays an important role in PDGF-induced VSMC migration in a copper-dependent manner.
- PDGF stimulation promotes ATP7A translocation from the *trans*-Golgi network (TGN) to the lipid raft microdomains which localize at the leading edge, thereby promoting lamellipodia formation through recruiting Rac1 as well as increasing lysyl oxidase (LOX) activity.
- In vivo, ATP7A expression is upregulated and copper accumulation is observed in neointimal VSMC in response to vascular injury.

Copper, an essential micronutrient, has been implicated in vascular remodeling in response to injury by unknown

mechanisms. Because excess copper is toxic, bioavailability of copper is tightly controlled not only by the copper importer CTR1, but also by the copper exporter ATP7A. Function of ATP7A is achieved through copper-dependent translocation from TGN. We investigated a role of ATP7A in PDGF-induced VSMC migration, a key component of neointimal formation after vascular injury. Here we show that depletion of ATP7A inhibits PDGF-induced VSMC migration in a copper/CTR1 dependent manner. Mechanistically, PDGF stimulation promotes ATP7A translocation from TGN to the lipid raft microdomains which localize at the leading edge in migrating VSMCs, thereby promoting lamellipodia formation through recruiting Rac1, as well as regulating LOX activity. In vivo, ATP7A is markedly increased in neointimal VSMC in wire injury model, in which copper accumulation is observed. Our findings uncover an unexpected role of ATP7A as a regulator of vascular migration in response to injury and provide insight into copper transporters as potential therapeutic targets for vascular remodeling and atherosclerosis. Furthermore, our studies will suggest a novel linkage between copper homeostasis and vascular migration.

## SUPPLEMENTAL MATERIAL

### Detailed Methods

**Materials:** Antibodies to PDGFR- $\beta$ , Rac1 (C-11, for immunoprecipitation) and paxillin were from Santa Cruz. Antibodies to caveolin-1 and Rac1 (for immunofluorescence) were from BD Biosciences Pharmingen. Rac1 antibody (for immunoblotting) and Rac/cdc42 Assay Reagent were from Millipore. Antibody against ATP7A was from Sigma-Aldrich, and antibodies against LOX-PP or LOX were from Novus Biologicals. Ctr1 antibody has been described previously<sup>1</sup>. Transwell 24-well plates were from BD Biosciences. Enhanced chemiluminescence (ECL) Western Blotting Detection Reagents and nitrocellulose membranes (Hybond-ECL) were obtained from Amersham Biosciences Corp. Oligofectamine, Opti-MEM I Reduced-Serum Medium, Alexa Fluor 568 phalloidin and Vybrant Lipid Raft Labeling Kit were from Invitrogen Corp. All other chemicals and reagents were from Sigma.

**Cell Culture:** Vascular smooth muscle cells (VSMCs) were isolated from male Sprague-Dawley rat thoracic aortas by enzymatic digestion<sup>2</sup>. Cells were grown in Dulbecco's modified Eagle's medium (DMEM) supplemented with 10% bovine serum and used at between passage 7 and 15. Cells were starved for 24 hours with serum free media before PDGF stimulation. For some experiments, VSMCs from other species, such as human aortic smooth muscle cells (HASMs) and mouse aortic smooth muscle cells (MASMs), were used. HASMs (Clonetics Corp) were cultured in smooth muscle basal medium (Clonetics) and 5% FBS. Experiments were performed using cells between passages 4 to 8.

MASMs were isolated from 8- to 10-week-old C57BL/6 mice (Jackson Laboratories) and cultured as previously described with modifications<sup>3,4</sup>. After removal of the connective tissue and blood, two aortas were incubated in an enzyme solution containing collagenase II (1.5 mg/mL), elastase (type II, 0.5 mg/mL), and trypsin inhibitor (type I-S, 1mg/mL) at 37°C. Cells were rinsed and plated in Dulbecco's modified Eagle's medium containing 10% FCS, glutamine (2 mmol/L), streptomycin (100 mg/mL), and penicillin (100 U/mL), and amphotericin B (25 mg/mL). The SMC identity of the cells was confirmed by staining with SMC-specific  $\alpha$ -actin monoclonal antibody (clone 1A4, Sigma Chemicals Inc). Experiments were performed using cells between passages 4 to 8.

**siRNA Transfection:** siRNAs were obtained from Applied Biosystem. VSMCs were seeded into culture dishes one day prior to transfection. Transfection of siRNA (30 nM) was performed using Oligofectamine (Invitrogen) according to the manufacturer's protocol. PDGF stimulation was performed 48 h after transfection.

**Reverse transcription-polymerase chain reaction (RT-PCR):** Total RNA was isolated from VSMCs using TRI reagent (Molecular Research Center, Inc) according to the manufacturer's instructions, and first stranded cDNA was synthesized with a High-Capacity cDNA Reverse Transcription Kits. The PCR was performed according to the manufacturer's protocol using ABI PRISM® 7000 Sequence Detection System (Applied Biosystems, CA) and QuantiFast SYBR Green PCR Kit (Qiagen, CA). PCR was performed with a 5 min preincubation at 95°C followed by 40 cycles of 10 s at 95°C and 30 s at 60°C. PCR products were subjected to melting curve analysis, using the ABI PRISM® 7000 Sequence Detection System, to exclude amplification of unspecific products, and separated on 2.5% agarose gel and stained with ethidium bromide. All real-time PCR primers were purchased from predesigned primers of QuantiTect primer assays (Qiagen).

**Scratch Wound Assay:** ATP7A, CTR1, or control siRNA-transfected VSMCs or BCS treated VSMCs were cultured on 6-well plates. Confluent cells were scraped using sterilized 10- $\mu$ L pipette tips and washed with 0.1% serum media, and stimulated with 50 ng/ml of PDGF for 24 h, as previously described<sup>5</sup>. Images were captured immediately at 0 h and at 24 h after the wounding.

**Modified Boyden Chamber Assay:** Migration assays using VSNCs with the Modified Boyden Chamber method were conducted in duplicate 24-well transwell chambers as described previously<sup>5</sup>. The upper insert (8- $\mu$ m pores coated with 0.1% gelatin) containing VSMCs suspensions ( $5 \times 10^4$  cells) transfected with ATP7A siRNA, CTR1 siRNA or control siRNA were placed in the bottom 24-well chamber containing fresh media with 0.2% FBS and stimulants. The chamber was incubated at 37°C for 8 h. The membrane was fixed and stained using Diff-Quick. Four random fields at  $\times 200$  magnifications were counted.

**Confocal Immunofluorescence Microscopy in VSMCs:** VSMCs on glass coverslips were rinsed quickly in ice-cold PBS, fixed in freshly prepared 4% paraformaldehyde in PBS for 10 min at room temperature, permeabilized in 0.05% Triton X-100 in PBS for 5 min, and rinsed sequentially in PBS, 50 m mol/L  $\text{NH}_4\text{Cl}$  and PBS for 10 min each. After incubation for 1 h in blocking buffer (PBS+3% BSA), cells were incubated with ATP7A antibody, PDGFR antibody, FITC-conjugated Rac1 antibody, Alexa Fluor 568-conjugated phalloidin for 18 h at 4°C, rinsed in PBS/BSA, and then incubated in either FITC-conjugated goat anti-IgY, rhodamine TRITC-conjugated donkey-IgY or Alexa Fluor 546-conjugated goat anti-rabbit IgG for 1 h at room temperature. Lipid rafts were stained with Vybrant Alexa Fluor 555 Lipid Raft Labeling kit. Cells on coverslips were mounted onto glass slides in Vectashield (Vector Laboratories) and examined using the 488 and 543 nm lines of the argon ion and green HeNe lasers. Controls with no primary antibody showed no fluorescence labeling and single label controls were performed in double labeling experiments.

For immunofluorescence staining of lipid rafts and F-actin in VSMCs, VSMCs on glass coverslips were stained with Vybrant Alexa Fluor 555 Lipid Raft Labeling kit, and then fixed in freshly prepared 4% paraformaldehyde in PBS for 10 min at room temperature, permeabilized in 0.05% Triton X-100 in PBS for 5 min, and rinsed sequentially in PBS, 50 m mol/l  $\text{NH}_4\text{Cl}$  and PBS for 10 min each. After incubation for 1 h in blocking buffer (PBS+3% BSA), cells were incubated with Alexa Fluor 488-conjugated phalloidin for 1 h at room temperature. Cells on coverslips were mounted onto glass slides in Vectashield and examined using the 488 and 543 nm lines of the argon ion and green HeNe lasers.

**Immunoprecipitation and Immunoblotting:** Growth-arrested cells were stimulated with PDGF at 37°C, and cells were lysed with 500  $\mu$ l of ice-cold lysis buffer, pH 7.4 (50 mM HEPES, 5 mM EDTA, 100 mM NaCl), 1% Triton X-100, 60 mM *n*-Octyl- $\beta$ -D-glucopyranoside, protease inhibitors (10  $\mu$ g/ml aprotinin, 1 mM phenylmethylsulfonyl fluoride, 10  $\mu$ g/ml leupeptin) and phosphatase inhibitors (50 mM sodium fluoride, 1 mM sodium orthovanadate, 10 mM sodium pyrophosphate). For immunoprecipitation cell lysates (1000  $\mu$ g) were precipitated with antibody overnight at 4°C and then incubated with 20  $\mu$ l of protein A/G-agarose beads for 1.5 h at 4°C. Cell lysates (25  $\mu$ g) or immunoprecipitates were separated using SDS-polyacrylamide gel electrophoresis and transferred to nitrocellulose membranes, blocked overnight in PBS containing 5% nonfat dry milk and 0.1% Tween 20, and incubated for overnight with primary antibodies as described previously. After incubation with secondary antibodies, proteins were detected by ECL chemiluminescence.

**Rac1 Activity Assay:** Rac activity was assessed with activity assay kit (Upstate Biotechnology) using a GST-conjugated PAK-1 protein-binding domain peptide, PAK-1 PBD, which binds only to Rac-GTP, according to manufacturer's instructions.

**Detergent-free Purification of Caveolin-rich Membrane Fractions:** Caveolae/lipid raft fractions were separated by the sodium carbonate-based detergent-free method <sup>6</sup>. Briefly, VSMCs were scraped into 2 ml of 500 mM sodium carbonate containing protease inhibitors (pH 11). Homogenization was carried out sequentially in the following order using a loose-fitting Dounce homogenizer (10 strokes) and a sonicator (four 20-s bursts). The homogenates were adjusted to 45% sucrose by adding 90% sucrose in a buffer containing 25 mM Mes (pH 6.5) and 0.15 M NaCl and placed at the bottom of an ultracentrifugation tube. A 5–35% discontinuous sucrose gradient was formed above and centrifuged at 39,000 rpm at 4°C for 16–20 h in a Beckman SW-40Ti rotor. From the top of the tube, 13 fractions were collected. Caveolae/lipid raft fractions were accumulated in fractions 4–6. These fractions contained <5% of total tissue protein content.

In some experiments, detergent-free OptiPrep gradient cell fractionation was also performed, as previously described <sup>7</sup>. Briefly, plasma membranes were isolated by Percoll gradient fractionation and then caveolae membranes were separated by two OptiPrep density gradients, a continuous 23% to 10% gradient followed by centrifugation against a discontinuous gradient to concentrate the lightest material. Proteins from each fraction were analyzed by Western Blotting.

**Copper Measurements by Inductively coupled plasma mass spectrometry (ICP-MS):** Samples were diluted to 2.0 ml with deionized water containing 5 % v/v nitric acid. The copper contents were analyzed by ICP-MS, using a PlasmaQuad3, as previously described <sup>8</sup>. Copper concentrations were calculated from calibration curves, and values for water blank were subtracted.

**Radioactive <sup>64</sup>Cu Uptake and Efflux Studies:** For copper uptake experiments, fresh serum free DMEM medium of 1.8 ml was added to the growth-arrested VSMCs, as described previously<sup>9</sup>. Cells were incubated for 30 min at 37 °C. Copper uptake was initiated by adding 200 µl of 10×CuCl<sub>2</sub> solution (20 µM) containing trace levels of <sup>64</sup>Cu (MIR radiological sciences, Washington University Medical School) and 50 ng/ml PDGF. Cells were incubated for 5 min (non-specific binding to the cells) or 30 min at 37 °C, and copper transport was terminated by the addition of ice-cold stop buffer (150 mM NaCl, 5 mM KCl, 2.5 mM MgCl<sub>2</sub>, 25 mM Hepes, pH 7.4, and 10 mM Na<sub>2</sub>-EDTA), after which cells were washed 3 additional times with ice-cold stop buffer. Cells were lysed using 0.1 M NaOH, and aliquots were counted using a liquid scintillation-counter (Beckman-Coulter LS6500). All transport determinations were carried out in triplicate. To exclude non-specific Cu uptake, the count of 5 min was subtracted from the count of 30 min. Copper uptake was then expressed as pmol of copper taken up by the cells per mg of protein after determination of the protein content of the cell monolayer by the Bio-Rad protein assay (Bio-Rad #500-0006). For copper efflux experiments<sup>10</sup>, cells were pulsed with 2 µM CuCl<sub>2</sub> solution containing trace levels of <sup>64</sup>Cu for 2 h, followed by three quick rinses with prewarmed serum free DMEM containing 2 µM CuCl<sub>2</sub> solution to remove any residual copper, and then incubated with prewarmed serum free DMEM containing 2 µM CuCl<sub>2</sub> solution and 50 ng/ml PDGF for several chase periods. Culture medium was collected at different time intervals and counted as above.

**Biotinylation of cell surface ATP7A and CTR1:** The cell surface ATP7A and CTR1 was biotinylated following exposure to VSMCs to 50 ng/ml of PDGF for indicated time. Biotinylation of cells was carried out using the cell-impermeable, thiol-cleavable Sulfo-NHS-SS-biotin (Pierce) reagent to label cell surface proteins, as previously described <sup>11</sup>. All of the biotinylation procedures

were carried out at 4 °C. Briefly, cell-surface proteins were labeled for 45 min with 0.2 mg/ml cleavable water-soluble cell-impermeant sulfo-NHS-SS-biotin (Pierce Endogen) in PBS supplemented with 0.5 mM MgCl<sub>2</sub> and 1 mM CaCl<sub>2</sub>. The unbound sulfo-NHS-SS-biotin was quenched by 50 mM Tris (pH 8.0) containing 100 mM NaCl. The cells were lysed in 500 µl of ice-cold lysis buffer, pH 7.4 (50 mM HEPES, 5 mM EDTA, 100 mM NaCl), 1% Triton X-100, 60 mM *n*-Octyl-β-D-glucopyranoside, protease inhibitors (10 µg/ml aprotinin, 1 mM phenylmethylsulfonyl fluoride, 10 µg/ml leupeptin) and phosphatase inhibitors (50 mM sodium fluoride, 1 mM sodium orthovanadate, 10 mM sodium pyrophosphate), and precipitated on streptavidin–agarose beads (Pierce Endogen) overnight. The beads were washed three times in lysis buffer, and were eluted in loading buffer. Proteins were subjected to Western immunoblot analysis to detect biotinylated ATP7A and CTR1 using anti-ATP7A or CTR1 antibodies.

**Vascular Injury and Morphometric Analysis:** Animal protocols were approved by the Animal Care and Use Committee of the University of Illinois at Chicago and University of Minnesota. Male ApoE deficient mice were fed a western diet for 2 weeks, followed wire injury, then continued western diet for 4 more weeks, euthanized, and collected injured arteries.

Wire-induced injury of the carotid artery in ApoE deficient atherosclerotic mice were performed, as described<sup>12</sup>. Briefly, mice were anesthetized using an intraperitoneal injection of ketamine (80 mg/kg body weight) and xylazine (5 mg/kg) (Phoenix Scientific, Inc., St. Joseph, MO). After midline neck incision, the left external carotid artery was tied off distally and a 0.014-inch flexible angioplasty guide wire was advanced by 1 cm along the common carotid artery via transverse arteriotomy. Complete and uniform endothelial denudation was achieved by five passes with a rotating motion. At different time points after injury, mice were anesthetized and perfused *in situ* using 4% paraformaldehyde at 100 mm Hg for tissue fixation. Injured arteries were excised and embedded in paraffin.

**Immunohistochemical analysis:** Paraffin-embedded tissue sections were stained with anti-ATP7A antibody (1:200), followed by a HRP-conjugated donkey anti-chicken IgY (1:100; Jackson ImmunoResearch). Staining was developed using the DAB Kit (Vector Laboratories, Burlingame, CA).

**Confocal Immunofluorescence Microscopy in tissues:** Paraffin-embedded tissue sections were stained with anti-ATP7A antibody (1:200) and anti-actin (for a smooth muscle isoform of actin) antibody (1:500), followed by a FITC-conjugated goat anti-IgY (1:100) and Rhodamine Red-conjugated goat anti-mouse IgG (1:50).

**Synchrotron X-ray Fluorescence Microscopy:** Sections (5 µm thick) of formalin-fixed paraffin-embedded wire-injured femoral artery were used. For X-ray imaging, the sections were mounted intact on silicon nitride windows (area, 2 × 2 mm; thickness, 200 nm) manufactured by Silson (Blisworth, U.K.) and attached by brief heating to 55°C, as previously described<sup>13</sup>. Specimens were imaged with the scanning X-ray fluorescence microprobe at beamline 2-ID-E of the Advanced Photon Source (Argonne, IL). Undulator-generated x-rays of 10-keV incident energy were monochromatized with a single bounce Si <111> monochromator and focused to a measured spot size of 0.3 × 0.5 µm using Fresnel zone plate optics (X-radia, Concord, CA). Sections were raster-scanned in steps of 4.0 µm, and fluorescence spectra were collected for 1- to 2-sec dwell times by using a single-element silicon drift detector (Vortex-EX, SII Nanotechnology, CA). Quantitation and image-processing of the X-ray fluorescence (XRF) data sets was performed with MAPS software<sup>14</sup>. Quantitation of elemental content was achieved by fitting XRF spectra at each pixel, and comparing

against a calibration curve derived from measurements of thin-film standards NBS-1832 and NBS-1833 (National Bureau of Standards, Gaithersburg, MD).

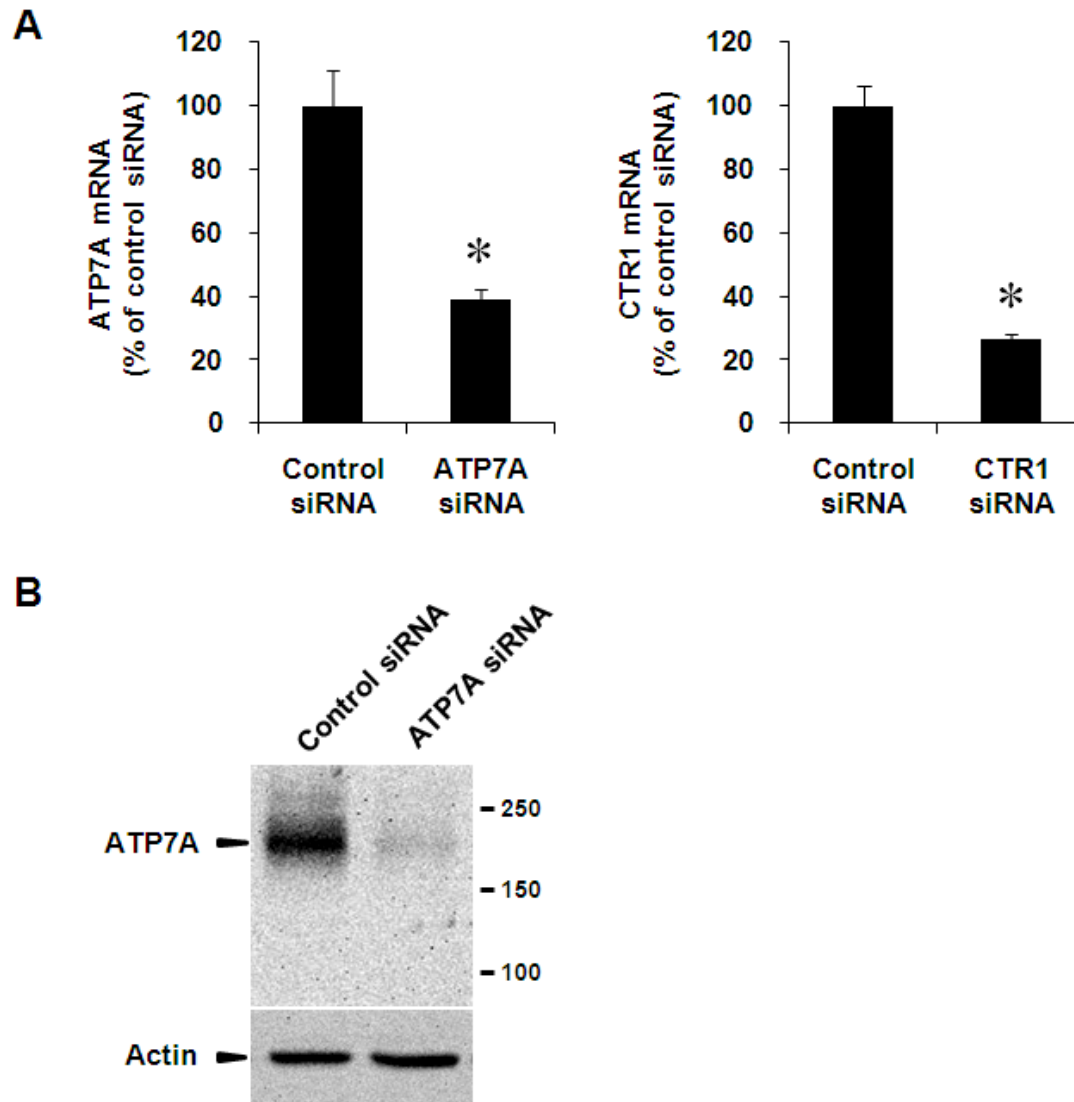
**Lysyl oxidase (LOX) activity assay.** LOX activity in cultured medium was measured by a high-sensitivity fluorescence assay as previously described<sup>15</sup>. Protein samples were incubated in the presence and absence of 500  $\mu\text{mol/L}$  BAPN at 37°C for 30 minutes with 1 U/mL horseradish peroxidase, 10  $\mu\text{mol/L}$  Amplex red (Molecular Probes), and 10 mmol/L 1,5-diaminopentane in 1.2 mol/L urea and 0.05 mol/L sodium borate (pH 8.2). The reaction was stopped on ice, and differences in fluorescence intensity (563-nm excitation wavelength and 587-nm emission wavelength) between samples with and without BAPN were determined. Results were normalized by cell protein content.

**Statistical analysis:** Statistical analysis was performed using the one-way analysis of variance (ANOVA), with the Scheffe test for post hoc comparisons when significance was determined by ANOVA or Student's *t*-test at the analysis indicated in the figures. The accepted level of significance was set at  $p < 0.05$ .

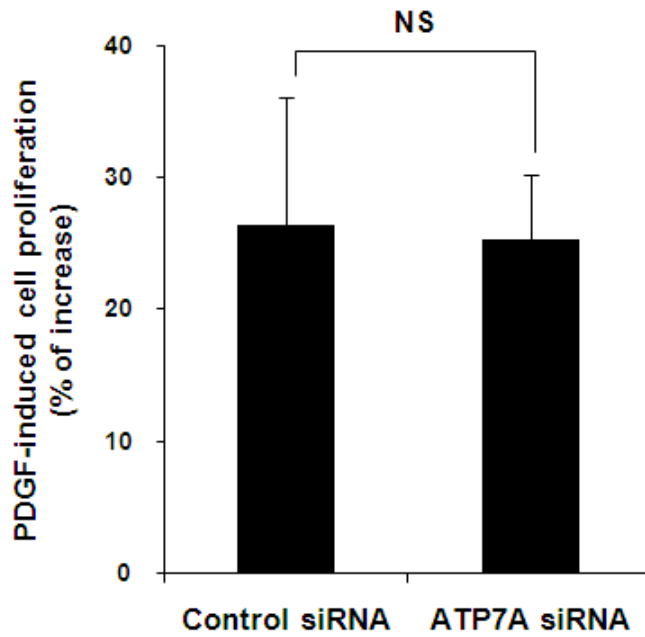
### Supplemental Reference

1. Maryon EB, Molloy SA, Kaplan JH. O-linked glycosylation at threonine 27 protects the copper transporter hCTR1 from proteolytic cleavage in mammalian cells. *J Biol Chem.* 2007;282:20376-20387.
2. Griendling KK, Taubman MB, Akers M, Mendlowitz M, Alexander RW. Characterization of phosphatidylinositol-specific phospholipase C from cultured vascular smooth muscle cells. *J Biol Chem.* 1991;266:15498-15504.
3. Mimura Y, Kobayashi S, Notoya K, Okabe M, Kimura I, Horikoshi I, Kimura M. Activation by alpha 1-adrenergic agonists of the progression phase in the proliferation of primary cultures of smooth muscle cells in mouse and rat aorta. *Biol Pharm Bull.* 1995;18:1373-1376.
4. Reddy MA, Li SL, Sahar S, Kim YS, Xu ZG, Lanting L, Natarajan R. Key role of Src kinase in S100B-induced activation of the receptor for advanced glycation end products in vascular smooth muscle cells. *J Biol Chem.* 2006;281:13685-13693.
5. Yamaoka-Tojo M, Ushio-Fukai M, Hilenski L, Dikalov SI, Chen YE, Tojo T, Fukai T, Fujimoto M, Patrushev NA, Wang N, Kontos CD, Bloom GS, Alexander RW. IQGAP1, a novel vascular endothelial growth factor receptor binding protein, is involved in reactive oxygen species--dependent endothelial migration and proliferation. *Circ Res.* 2004;95:276-283.
6. Song KS, Li S, Okamoto T, Quilliam LA, Sargiacomo M, Lisanti MP. Co-purification and direct interaction of Ras with caveolin, an integral membrane protein of caveolae microdomains. Detergent-free purification of caveolae microdomains. *J Biol Chem.* 1996;271:9690-9697.
7. Smart EJ, Ying YS, Mineo C, Anderson RG. A detergent-free method for purifying caveolae membrane from tissue culture cells. *Proc Natl Acad Sci U S A.* 1995;92:10104-10108.
8. Jeney V, Itoh S, Wendt M, Gradek Q, Ushio-Fukai M, Harrison DG, Fukai T. Role of antioxidant-1 in extracellular superoxide dismutase function and expression. *Circ Res.* 2005;96:723-729.
9. Eisses JF, Kaplan JH. Molecular characterization of hCTR1, the human copper uptake protein. *J Biol Chem.* 2002;277:29162-29171.
10. Hamza I, Faisst A, Prohaska J, Chen J, Gruss P, Gitlin JD. The metallochaperone Atox1 plays a critical role in perinatal copper homeostasis. *Proc Natl Acad Sci U S A.* 2001;98:6848-6852.
11. Molloy SA, Kaplan JH. Copper-dependent recycling of hCTR1, the human high affinity copper transporter. *J Biol Chem.* 2009;284:29704-29713.
12. Wang H, Zhang W, Tang R, Hebbel RP, Kowalska MA, Zhang C, Marth JD, Fukuda M, Zhu C, Huo Y. Core2 1-6-N-glucosaminyltransferase-I deficiency protects injured arteries from neointima formation in ApoE-deficient mice. *Arterioscler Thromb Vasc Biol.* 2009;29:1053-1059.
13. Finney L, Mandava S, Ursos L, Zhang W, Rodi D, Vogt S, Legnini D, Maser J, Ikpatt F, Olopade OI, Glesne D. X-ray fluorescence microscopy reveals large-scale relocalization and extracellular translocation of cellular copper during angiogenesis. *Proc Natl Acad Sci U S A.* 2007;104:2247-2252.

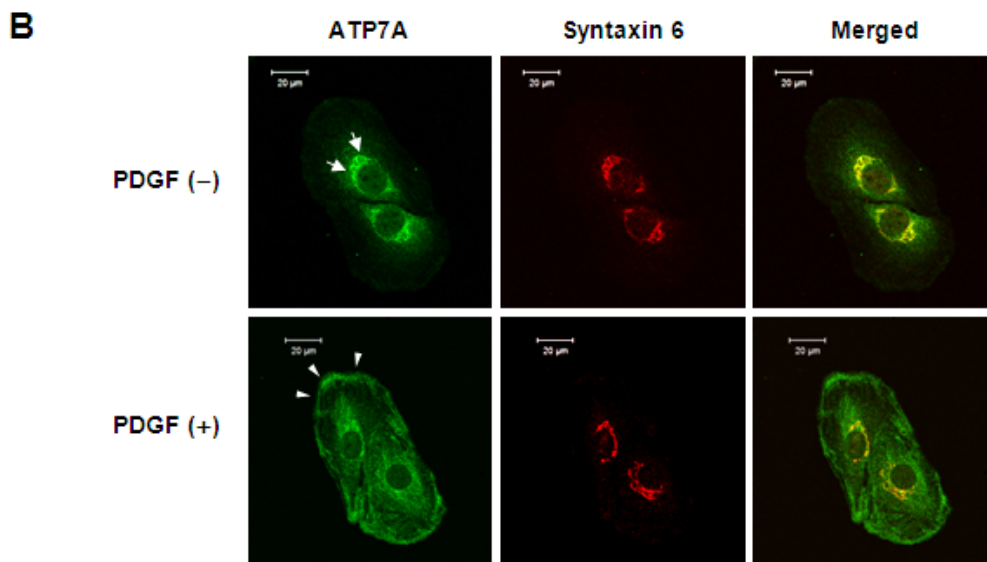
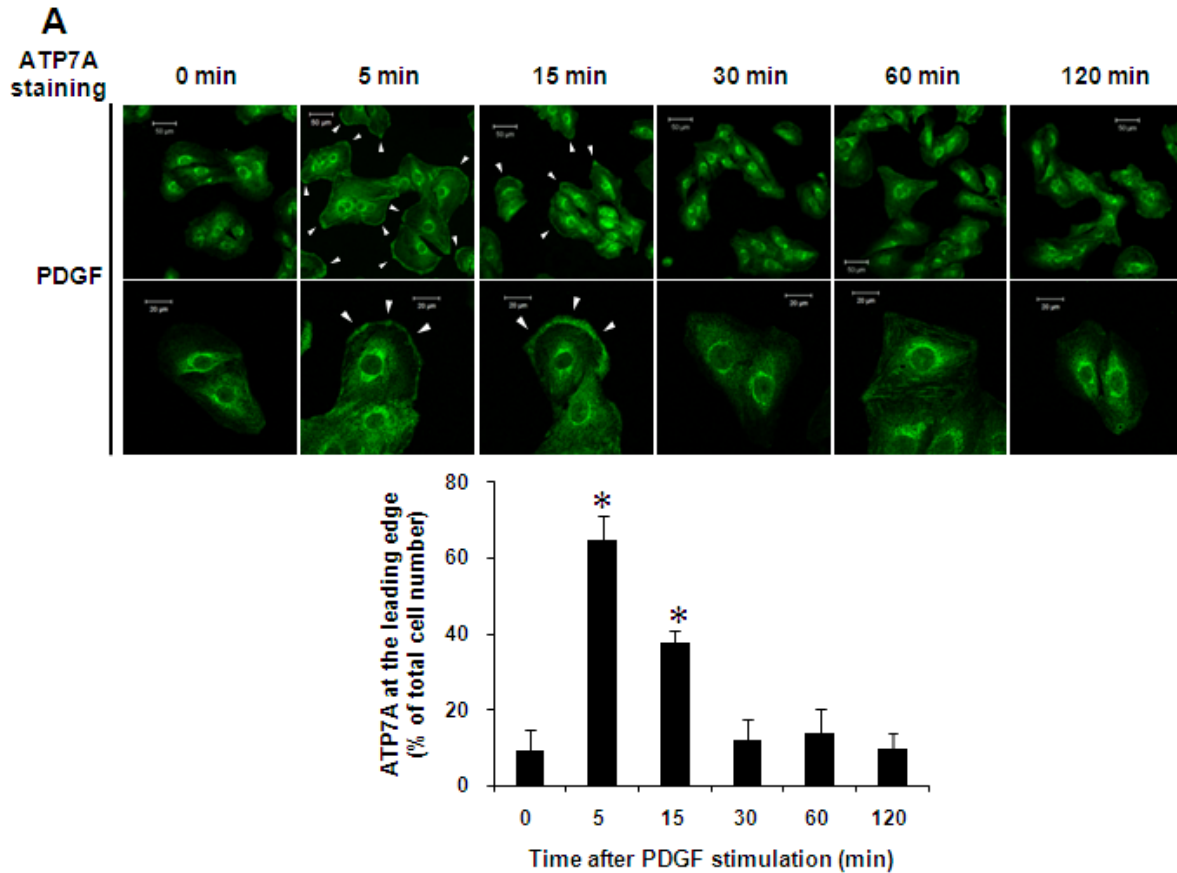
14. Vogt S. MAPS: A set of software tools for analysis and visualization of 3D X-ray fluorescence data sets. *J Phys IV*. 2003;104:635-638.
15. Palamakumbura AH, Trackman PC. A fluorometric assay for detection of lysyl oxidase enzyme activity in biological samples. *Anal Biochem*. 2002;300:245-251.
16. Itoh S, Kim HW, Nakagawa O, Ozumi K, Lessner SM, Aoki H, Akram K, McKinney RD, Ushio-Fukai M, Fukai T. Novel role of antioxidant-1 (Atox1) as a copper-dependent transcription factor involved in cell proliferation. *J Biol Chem*. 2008;283:9157-9167.
17. Lee J, Petris MJ, Thiele DJ. Characterization of mouse embryonic cells deficient in the ctr1 high affinity copper transporter. Identification of a Ctr1-independent copper transport system. *J Biol Chem*. 2002;277:40253-40259.
18. Tang SS, Trackman PC, Kagan HM. Reaction of aortic lysyl oxidase with beta-aminopropionitrile. *J Biol Chem*. 1983;258:4331-4338.



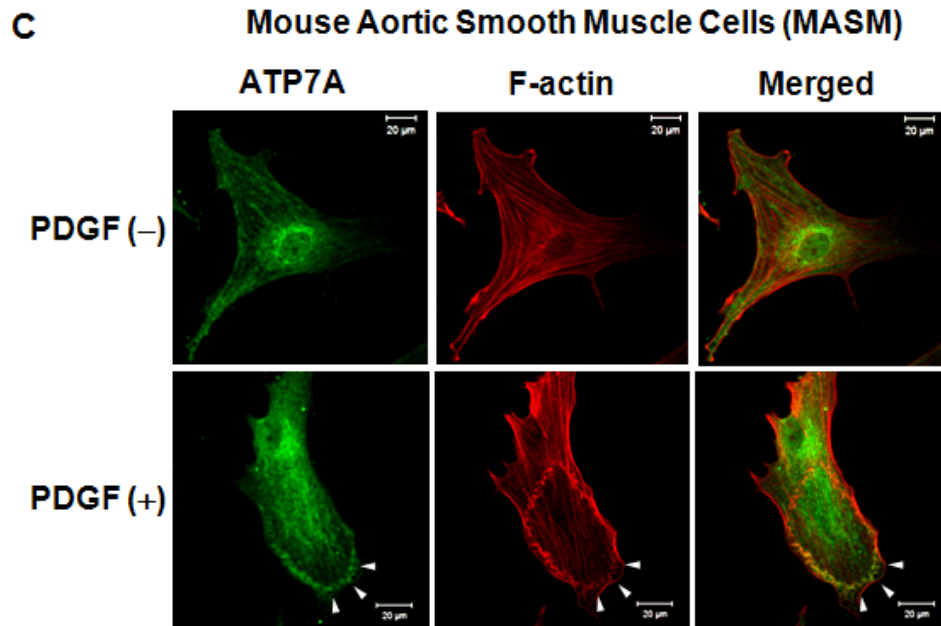
**Online Figure I:** siRNA-mediated knockdown of endogenous ATP7A and CTR1 expression in VSMCs. **A**, Real-time PCR analysis of total RNA extracted from RASMs transfected with either ATP7A, CTR1, or control siRNA. **B**, Western-blot analysis of total cell lysates from RASMs transfected with either ATP7A or control siRNA, using anti-ATP7A (upper) and anti-actin (lower) antibodies. Actin was used as a loading control.



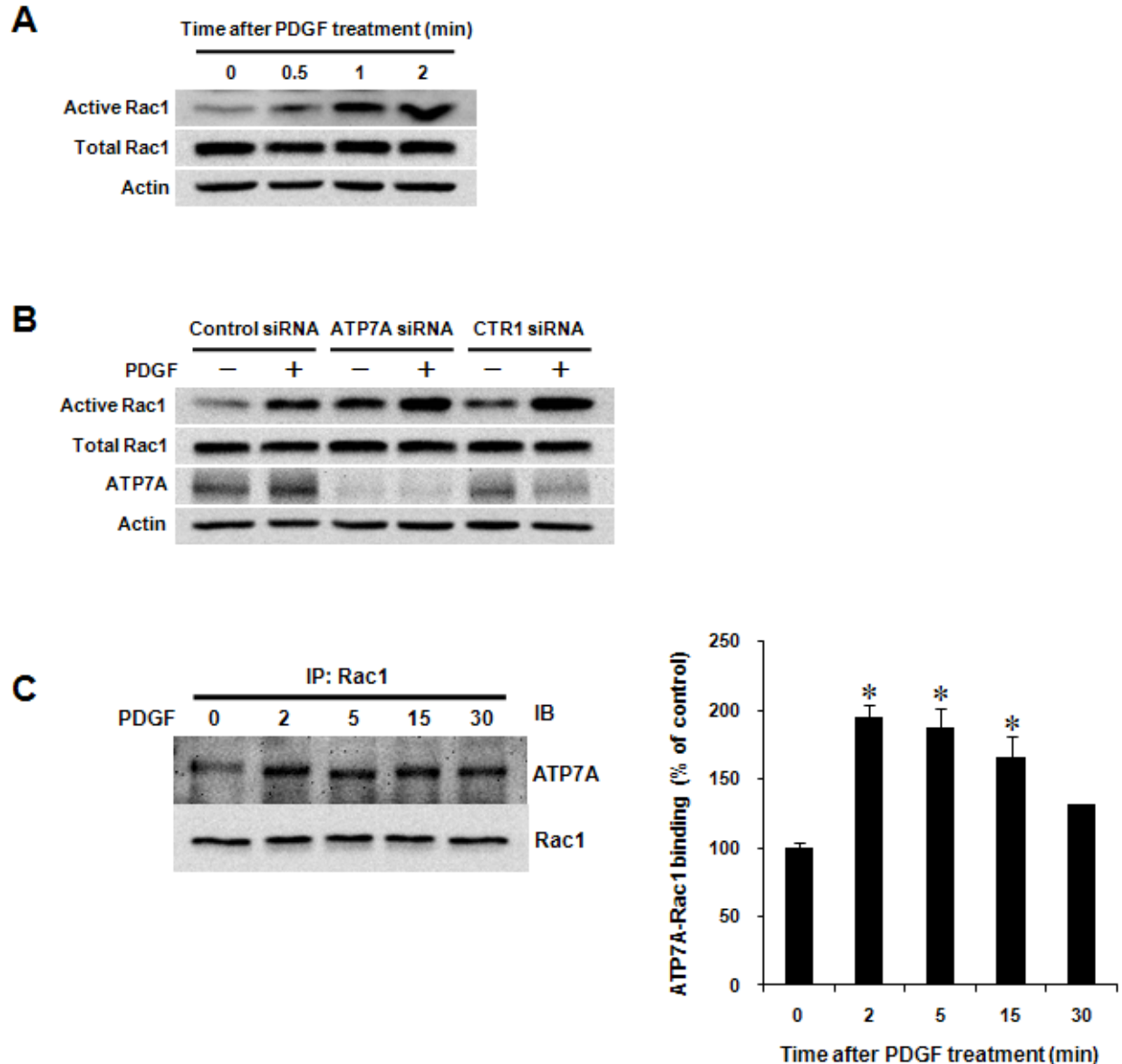
**Online Figure II:** Effect of ATP7A siRNA on PDGF-induced VSMC proliferation. Cell proliferation stimulated with or without 50 ng/ml of PDGF in RASMs was determined by cell number after plating cells in 0.1 % bovine serum containing culture medium for 72 hour, as previously described<sup>5,16</sup>. Values are the mean  $\pm$  S.D. for 3 independent experiments. *NS*, not significant.



**Online Figure III:** PDGF stimulation promoted ATP7A translocation from transGolgi network (TGN) to the plasma membrane leading edge in VSMCs. **A**, Growth-arrested RASMs were stimulated with 50 ng/ml PDGF for indicated time, and cells were stained for ATP7A. **B**, Growth-arrested RASMs were stimulated with or without 50 ng/ml PDGF, and cells were co-stained for ATP7A and syntaxin 6, a TGN marker. Small white arrowheads point to the plasma membrane leading edge, while white arrows point to TGN (PDGF (-) cells). Results are representative of 3 independent replicates of immunofluorescence images.

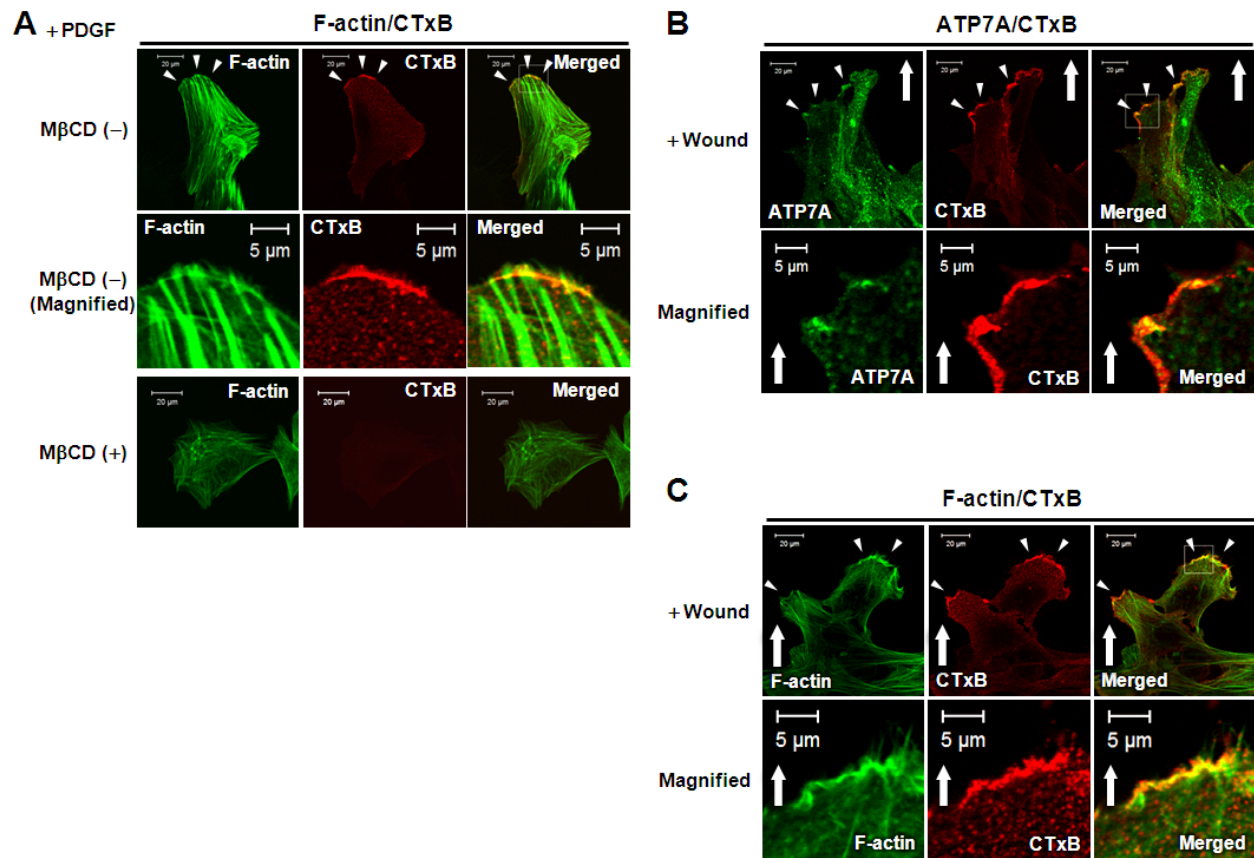


**Online Figure III: C,** ATP7A is translocated to the leading edge in MASMs stimulated by PDGF. Growth-arrested MASMs were stimulated with or without 50 ng/ml PDGF for 5 min in a similar fashion to Figure 2. Cells were co-stained with ATP7A and phalloidin. Small white arrowheads point to the leading edge and large arrows point to direction of migration.

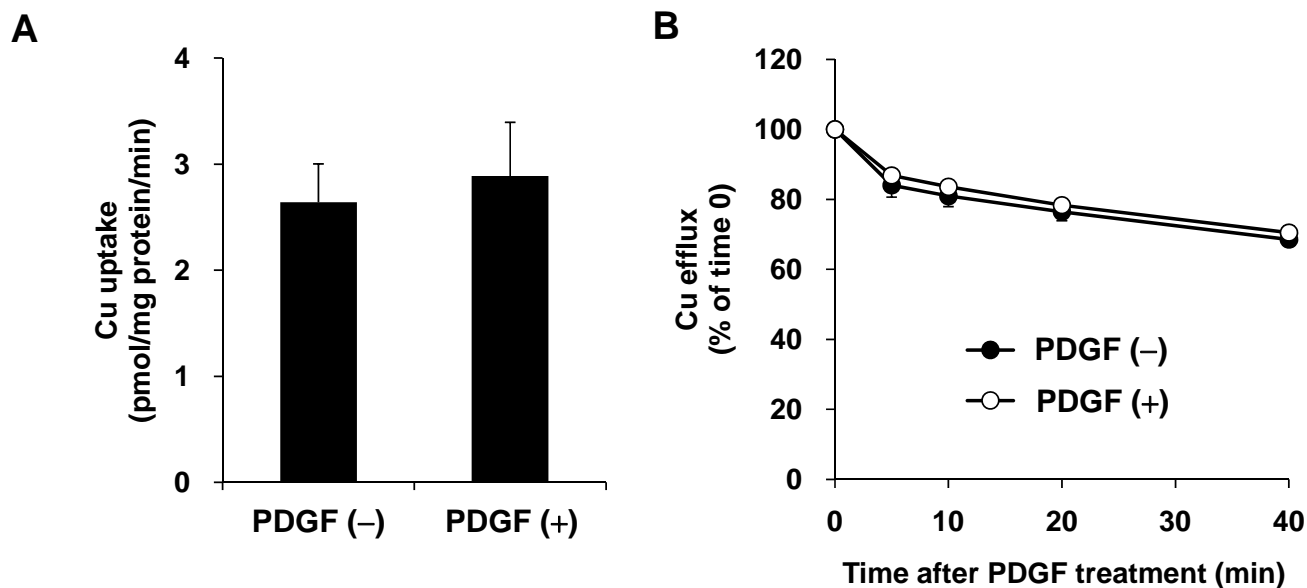


**Online Figure IV:** PDGF stimulation increased active, GTP-bound form of Rac1 within 1 min, which was not affected by either ATP7A or CTR1 siRNA. **A**, Effect of PDGF on Rac1 activation. Growth-arrested RASMs were stimulated with 50 ng/mL of PDGF for indicated times (min). Lysates bound to p21-activated kinase 1 agarose were immunoblotted with anti-Rac antibody. **B**, Effect of ATP7A or CTR1 siRNA on PDGF induced Rac1 activation. Growth-arrested RASMs transfected with ATP7A, CTR1, or control siRNA were stimulated with 50 ng/mL of PDGF for 2 min. Lysates bound to p21-activated kinase 1 agarose were immunoblotted with anti-Rac antibody. **C**, PDGF stimulation promoted Rac1 association with ATP7A in a time-dependent manner. Growth-arrested RASMs was stimulated with 50 ng/mL of PDGF for indicated times (min). Lysates were IP with anti-Rac1 antibody, followed by IB with ATP7A.

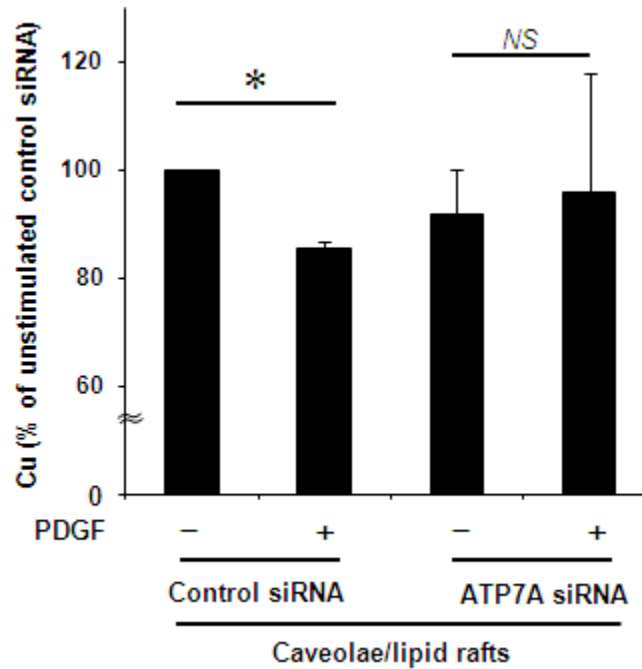




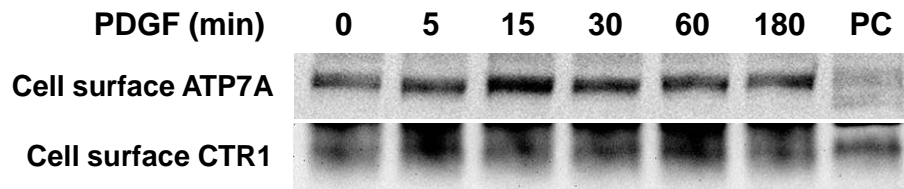
**Online Figure VI:** ATP7A is translocated to the lipid rafts localized at the leading edge in actively migrating VSMCs, thereby promoting lamellipodia formation. **A**, CTxB accumulated and colocalized with F-actin at the leading edge in PDGF stimulated VSMCs. Growth-arrested RASMs were treated with or without 10 mM of methyl- $\beta$ -cyclodextrin for 2 h, and stimulated with 50 ng/mL of PDGF for 5 min. VSMCs were stained with phalloidin (green) and cholera toxin subunit B (CTxB) (red). All fluorescence images were taken at 5 different fields/well, and the cell images are representative of more than 3 different experiments. **B and C**, ATP7A is translocated to the lipid rafts localized at the leading edge in VSMCs after wound scratch, thereby promoting lamellipodia formation. Growth-arrested confluent monolayer of RASMs were stained with either anti-ATP7A antibody (green) and cholera toxin subunit B (CTxB)-Alexa 555 (red) (B) or phalloidin (green) and cholera toxin subunit B (CTxB)-Alexa 555 (red) (C) after wound scratch in the presence of PDGF for 18 hours. Small white arrowheads point to the leading edge and large arrows point to direction of migration. All fluorescence images were taken at 5 different fields/well, and the cell images are representative of more than 3 different experiments.



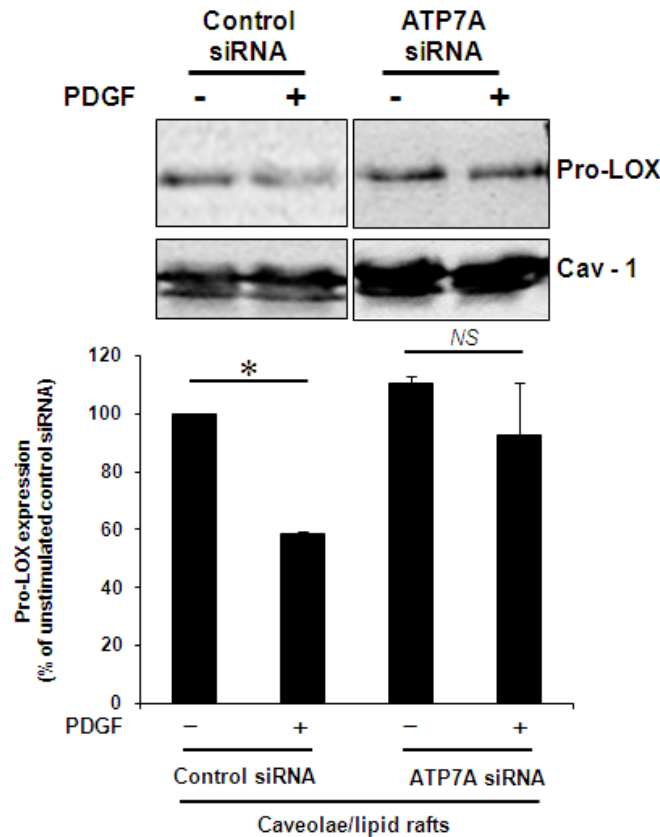
**Online Figure VII:** Copper-uptake and efflux assessed by  $^{64}\text{Cu}$  copper transport assays were not altered by PDGF in VSMCs. **A**,  $^{64}\text{Cu}$  uptake assays in PDGF stimulated VSMCs. Growth-arrested RASMs were treated with  $2\ \mu\text{M}$   $\text{CuCl}_2$  containing trace levels of  $^{64}\text{Cu}$  and  $50\ \text{ng/ml}$  PDGF. Cells were incubated for 5 min (non-specific binding to the cells) or 30 min at  $37\ ^\circ\text{C}$ . Uptaken  $^{64}\text{Cu}$  was counted using a  $\gamma$ -counter. **B**,  $^{64}\text{Cu}$  efflux assays in PDGF stimulated VSMCs. Growth-arrested RASMs were pulsed with  $2\ \mu\text{M}$   $\text{CuCl}_2$  solution containing trace levels of  $^{64}\text{Cu}$  for 2 h, followed by rinses with prewarmed serum free DMEM containing  $2\ \mu\text{M}$   $\text{CuCl}_2$  solution, and then incubated with prewarmed serum free DMEM containing  $2\ \mu\text{M}$   $\text{CuCl}_2$  solution and  $50\ \text{ng/ml}$  PDGF for several chase periods. Culture medium was collected at different time intervals and counted using a  $\gamma$ -counter. The results shown here are the means  $\pm$  S.D. for a single experiment and are representative of those obtained from three independent experiments.



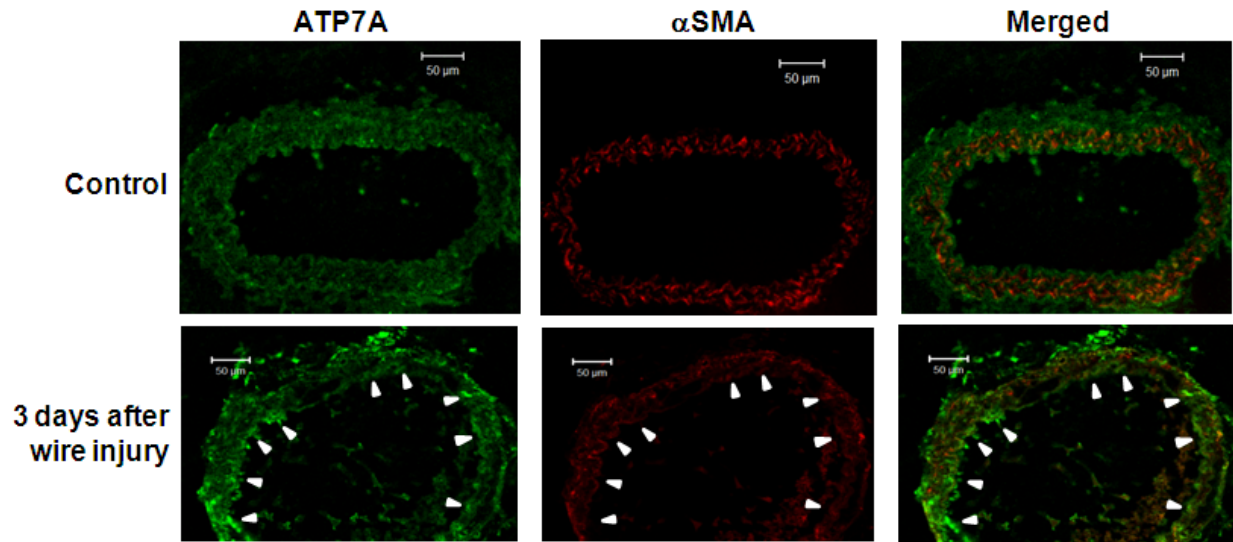
**Online Figure VIII: PDGF stimulation reduces copper content in caveolae/lipid raft fractions in an ATP7A-dependent manner in VSMCs.** Copper contents were measured by inductively coupled plasma mass spectrometry (ICP-MS) in caveolae/lipid rafts in RASMs transfected with ATP7A or control siRNA, followed by stimulated with or without PDGF for 5 min. Equal amount of proteins in caveolae/lipid rafts (fraction 4-5) were obtained by sucrose gradient fractionation as described in Figure 5. (Mean  $\pm$ S.D. n=3) \* $p$ <0.05 vs. unstimulated cells.



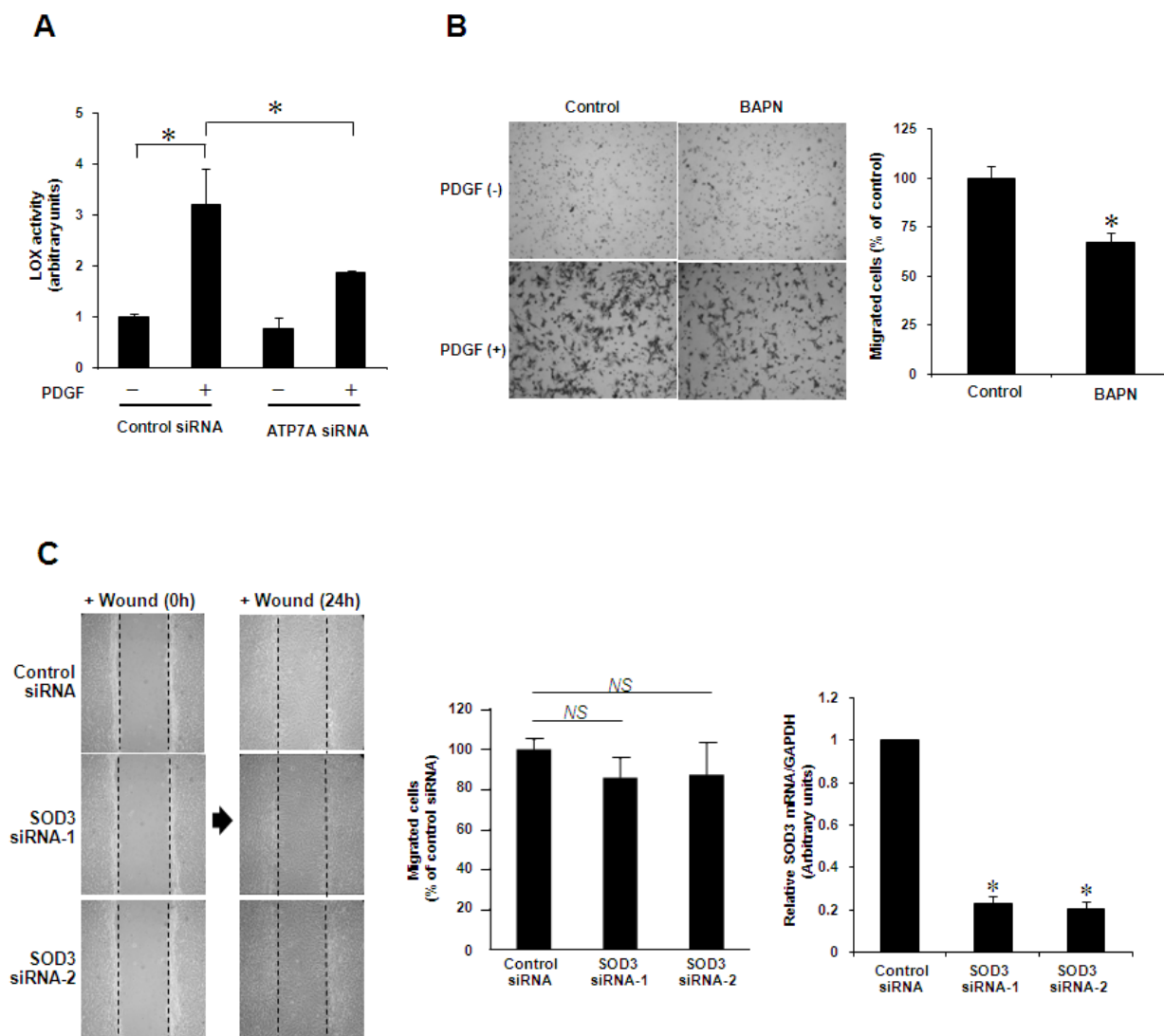
**Online Figure IX:** Plasma membrane localization of ATP7A and CTR1 in PDGF-stimulated VSMCs using cell surface biotinylation assays. The cell surface ATP7A and CTR1 was biotinylated following exposure to RASMs to 50 ng/mL of PDGF for indicated time. Biotinylated proteins were precipitated using streptavidin-agarose beads and separated by SDS/PAGE as described in the Method section. Biotinylated ATP7A and CTR1 were detected by Western-blotting using anti-ATP7A and CTR1 antibodies.



**Online Figure X: PDGF stimulation decreases Pro-LOX level in lipid raft fractions in an ATP7A-dependent manner in VSMCs.** Equal amounts of proteins in caveolae/lipid rafts (fraction 4-5) were immunoblotted with anti-LOX-PP or caveolin-1 antibodies. RASMs were transfected with CTR1 or control siRNA, followed by stimulated with or without 50 ng/ml of PDGF for 5 min. Sucrose gradient centrifugation was performed as described in Figure 5. Right panel shows averaged data for ATP7A protein, expressed as % of unstimulated, control siRNA-treated VSMCs (means  $\pm$  S.D, n=3). \* $p$ <0.05 vs. control siRNA-treated cells.



**Online Figure XI. Immunofluorescence analysis for uninjured (control) or injured (3 days after) carotid arteries of ApoE-deficient atherosclerotic mice.** Vessels were co-stained with anti- ATP7A (green) and  $\alpha$ -smooth muscle actin (red) antibodies.



**Online Figure XII:** **A**, Role of ATP7A in lysyl oxidase (LOX) activity in VSMCs. RASMs were transfected with control siRNA or ATP7A siRNA with or without PDGF treatment. LOX secreted in the culture medium was collected at 48-hour after addition of PDGF (50ng/ml). Its activity was measured by the oxidation of Amplex Red (Invitrogen) in the presence of 1,5-diaminopentane substrate, as previously described<sup>15</sup>. The results are presented as mean  $\pm$  SE from 3 separate experiments. \*  $P < 0.01$  vs. control siRNA cells with or without PDGF treatment. **B**, Role of LOX activity in VSMC migration. RASMs were treated with beta-aminopropionitrile (BAPN)(100uM for 24h), an irreversible inhibitor of lysyl oxidase activity<sup>18</sup>. Cell migration was assessed by the modified Boyden chamber assay after stimulation with or without 50 ng/ml of PDGF for 8 hours. Bar graph represents averaged data, expressed as cell number per field. \* $p < 0.05$  vs. untreated cells. Values are the mean  $\pm$  S.D. for 3 independent experiments. **C**, Role of SOD3 in VSMC migration. Wound scratch assay was performed in confluent monolayers of RASMs transfected with siRNA (two kinds of SOD3 siRNAs, or control siRNA) in the presence of PDGF (50 ng/ml), as described in Figure 1E. Images were captured immediately after rinsing at 0 h and at 24 h after the wounding in the cells. Bar graph represents averaged data, expressed as cell number per field. \* $NS$  vs. control siRNA-treated cells. Values are the mean  $\pm$  S.D. for 3 independent experiments.